

Authors' response to Referee 1

Journal : Ocean Sciences

Paper title: Impact of intraseasonal wind bursts on SST variability in the far eastern Tropical Atlantic Ocean during boreal spring 2005 and 2006. Focus on the mid-may 2005 event.

Authors: Herbert Gaëlle, Bourlès Bernard.

We thank Reviewer 1 for his comments and suggestions.

RC: Reviewer's comment; **AC**: Authors' comment; **MC**: Manuscript changes

RC: I appreciate the authors' effort in addressing the issues raised in my review. I find the revised manuscript to be improved, but there are still a number of things that need to be taken care of before publication. In particular, I find that my major comments 1 and 2 and specific comments 1, 4, 5, 8, 10, 11, and 12 have been adequately addressed. Regarding the other comments, I still have the following concerns:

1. **RC**: A) With respect to the different time scales (related to former major comment 1 and specific comment 2 and 7), I am still having difficulty to sort out the relationship between the intraseasonal and interannual anomalies. The authors did not make it easier for me with their replies that completely mix up the time scales (AC to major comment 3 states that Fig. 4 shows interannual anomalies, the figure caption itself says intraseasonal; AC to specific comment 2 talks about interannual anomalies, but the manuscript change is about intraseasonal variations). I would strongly advise the authors to define and cleanly separate the time scales and ideally draw a conclusion how the intraseasonal episodes lead to the interannual cold event in 2005.

AC & MC: Thanks for the comment. We apologize for the confusion. Indeed, there was a mistake in our reply to major comment 3 and to specific comment 2. We wanted to say "intraseasonal" and not "interannual". Fig.4 shows intraseasonal anomalies. The text about Fig. 3 & 4 has been modified and comments about the year 2006 have been added, as follows (section 4.1):

"The cooling episodes occurred east of 5° E from April to September. In 2005, the intraseasonal cooling episodes took place on 8-12 May, 16-22 May, 30 May-June 6, and 12-16 June, whereas in 2006 they took place on 20-30 April, 14-24 May, 14-20 & 26-30 June. The temperature drop for the two years ranged between -0.2°C to -2°C."

The interannual variability is highlighted in Section 3. Then, the paper focuses on intraseasonal SST and southerly wind anomalies. This point is briefly addressed at the end of the section 4.1:

“Besides, model SST fields (Fig. 3a) indicate that the SST minimum (~24° C) in 2005 was reached in July, i.e. one month earlier than in 2006, as also noticed in seasonal variations of SST averaged in the region (Fig. 1a). These results illustrate the important role of the succession of quick and intense cooling episodes in the establishment of persistent cold anomalies in the CLR, as highlighted by Marin et al. (2009) in the equatorial region.”

The different processes implied in the occurrence of cooling episodes in boreal spring and the cause of differences observed from year to year are summarized in the conclusion :

“In the CLR, stronger wind intensification and favorably preconditioned oceanic subsurface conditions in 2005 made the coupling between surface and subsurface ocean processes more efficient than in 2006, resulting in stronger cooling. It should be noted that the occurrence of intraseasonal wind intensification in the CLR is not specific to the boreal spring/summer 2005 and 2006 and is observed every year over the 1998-2008 period of study (not shown). However, their impact on SST variability in the region is modulated depending of the strength of wind intensification and of the subsurface preconditioning. For example, the year 1998, known as a “warm year”, is characterized by anomalous warm SST in boreal spring/summer in the CLR., associated with anomalous weak winds and anomalous deep thermocline.”

2.RC: B) line 196/197: The highest temperatures occur more towards boreal spring than winter (former specific comment 3). The AC states that the text has been modified, but it has not.

AC & MC: Sorry for that, the text has been modified as follows: *“The SST variations display an annual cycle with highest temperature at the end of boreal winter – beginning of boreal spring [...]”*

3.RC: C) I appreciate that Figures 3 and 4 have been revised. However, I still find it impossible to identify the individual dates of cooling episodes and wind bursts that are given in the text in those figures (former specific comment 6). Maybe you could highlight those dates by vertical lines or arrows?

AC: Black brackets and light grey lines have been added on Fig.3 in order to highlight the cooling episodes. On Fig.4, shaded areas have been added for highlight the dates of the wind bursts. Then, the labels have been enlarged.

4.RC: D) Regarding the seasonality of the upwelling (lines 205 to 208, 228), I believe that the passage of coastal Kelvin waves plays an important role as well (e.g. Ostrowski et al., 2009).

AC & MC: Tanks for the comment. We slightly modified the text as follows:

“The SST May-June average map indicates that the boreal summer SST minimum is related to intensified cool SST around 6°S, in the Congo mouth region. In this region, the coast is oriented parallel to the trade flow which reinforces in boreal summer, thus favorable to

coastal upwelling processes. The mean alongshore wind stress during May-June reveals in fact that upwelling conditions are observed over most of the CLR. The coastal upwelling could also interact with the coastal Kelvin wave propagation (e.g. Ostrowski et al., 2009) highlighted by minimum z_{20} values in Fig. 1d

5.RC: E) Despite some improvements, many of the figures are still very small with labels that are hard to read. I also find that the “rainbow” colormap is not ideal for showing anomalies and would advise to use a colormap centered around white or very light colors instead.

AC: Thanks for the suggestion. The labels of Fig.3, 4, 5, 6, 7, 8, 9, 10, 11, 12 have been enlarged.

6.RC: In Fig. 11b, the colormap is not very instructive either.

AC: The colormap of Fig. 11b has been modified.

7.RC: For Fig. 12, the caption is not consistent with the labels of the subplots regarding the order of wind stress and radiation.

AC: The colormap of the subplot showing the radiation has been modified.

8.RC: Figure 2 is still mentioned for the first time in the text after Figure 3.

AC: Sorry for that. We have added a reference to the Fig. 2 in the Introduction, as follows:

“The question of the processes implied in the SST variability in the Cape-Lopez region was raised based on an observation in satellite SST data of cold coastal waters during boreal spring independent from those observed off shore in the cold tongue region around 10°W (see Fig. 2) which also raised the question of the link of such cooling with the cold tongue development.”

9.RC: F) There are also still a number of language issues. I have made some suggestions below (quite a few of them not for the first time, I believe...) but the manuscript would probably benefit from a careful read-through by a native English speaker.

AC: Thanks for pointing the technical corrections. The corrections have been made.

Authors' response to Referee 2

Journal : Ocean Sciences

Paper title: Impact of intraseasonal wind bursts on SST variability in the far eastern Tropical Atlantic Ocean during boreal spring 2005 and 2006. Focus on the mid-may 2005 event.

Authors: Herbert Gaëlle, Bourlès Bernard.

We thank Reviewer 2 for his comments.

RC: Reviewer's comment; **AC**: Authors' comment; **MC**: Manuscript changes

RC: The authors have taken all of the reviewers' comments into account and, in my opinion, have addressed them sufficiently and made appropriate changes to the manuscript. I do still think this paper would benefit from having a native English speaker review it, though it is much better in this version. That said, the few places that still need correction do not detract from the meaning of the sentences, and the reader is able to follow along easily.

AC: Thanks for your comments. Many technical corrections have been made in the revised version.

Authors' response to Referee 3

Journal : Ocean Sciences

Paper title: Impact of intraseasonal wind bursts on SST variability in the far eastern Tropical Atlantic Ocean during boreal spring 2005 and 2006. Focus on the mid-may 2005 event.

Authors: Herbert Gaëlle, Bourlès Bernard.

We thank Reviewer 3 for his comments and suggestions.

RC: Reviewer's comment; **AC**: Authors' comment; **MC**: Manuscript changes

1.RC: line 248: I don't see the April 22-24 cooling event in Fig. 4a. The others that you list are visible.

AC&MC: Thanks for the remark. Indeed, this is a mistake. The text has been modified and comments about the year 2006 have been also added, as follows:

“The cooling episodes occurred east of 5° E from April to September. In 2005, the intraseasonal cooling episodes took place on 8-12 May, 16-22 May, 30 May-June 6, and 12-16 June, whereas in 2006 they took place on 20-30 April, 14-24 May, 14-20 & 26-30 June. The temperature drop for the two years ranged between -0.2°C to -2°C.”

In addition, for more clarity, black brackets have been added on Fig.3 to indicate the dates of the cooling episodes, and shaded areas have been added in Fig.4 to indicate the southerly wind events.

2. RC: line 289: “Globally” is not the right word to use here. I would simply delete it.

AC: Thanks for the suggestion. It has been deleted.

3.RC: line 340: You discuss the shallower thermocline being more conducive to anomalous cooling, which is probably true for vertical mixing induced by current shear and wind. However, the heat capacity (i.e., mixed layer depth) can also have a big impact on the change in SST for given heat flux, and it is not necessarily correlated with thermocline depth. I suggest checking to see if MLD follows Z20, or at least adding a disclaimer that Z20 is not necessarily the same as MLD.

AC & MC: We have slightly modified the text as follows:

“As previously shown, the time of occurrence of the cold events in the CLR coincides with shallow thermocline which contributes to making the mixed layer temperature more reactive to surface forcing (note that z20 is not necessarily the same as the mixed layer depth).”

4.RC: Fig. 7: I suggest reversing the y axis in Fig. 7e,k so that shallow Z20 anomalies are up instead of down.

AC & MC: Thanks for the suggestion. However, this would be in contradiction with another reviewer's comment. For more clarity, the line below has been added in the legend of the Fig. 7: *“Negative values indicate a 20°C isotherm depth closer to the surface”*

5.RC: line 416: How does Ekman convergence reinforce upwelling? Do you mean divergence?

AC: Yes, we mean divergence. This has been corrected in the text.

6. RC: Fig. 9: It's a little confusing to have the longitude on the y axis (longitude goes across, not up and down like latitude). Consider putting it on the x axis and making columns instead of rows.

AC: Thanks for the suggestion. The Fig. 9 has been modified.

7.RC: line 580: Change 'humidify' to 'humidity'

AC: Thanks. The modification has been made.

There are numerous mostly minor language/grammatical errors that need to be corrected. It's not a major thing, but they are distracting when reading the text.
Many corrections have been made.

In addition, the labels of most of the figures have been enlarged.

1 **Impact of intraseasonal wind bursts on SST variability in the**
2 **far eastern Tropical Atlantic Ocean during boreal spring**
3 **2005 and 2006. Focus on the mid-May 2005 event.**

4 Gaëlle Herbert¹, Bernard Boulès¹

5 ¹:Institut de Recherche pour le Développement (IRD), Laboratoire d'Etudes Géophysiques et Océanographie Spatiale
6 (LEGOS), Brest, France.

7 *Correspondence to:* Gaëlle Herbert (gaelle.herbert@ird.fr)

8

9 **Abstract.** The impact of boreal spring intraseasonal wind bursts on sea surface temperature variability in the
10 eastern Tropical Atlantic Ocean in 2005 and 2006 is investigated using numerical simulation and observations.
11 We specially focus on the coastal region east of 5° E and between the equator and 7° S that has not been studied
12 in detail so far. For both years, the southerly winds **anomalies** induced cooling episodes through i) upwelling
13 processes; ii) vertical mixing due to vertical shear of the current; and for some particular events iii) a decrease
14 of incoming surface shortwave radiation. The strength of the cooling episodes was modulated by subsurface
15 conditions affected by the arrival of Kelvin waves from the west influencing the depth of the thermocline. Once
16 impinging the eastern boundary, the Kelvin waves excited westward-propagating Rossby waves which,
17 combined with the effect of enhanced westward surface currents, contributed to the westward extension of the
18 cold water. A particularly strong wind event occurred in mid-May 2005 and caused an anomalous strong cooling
19 off Cape-Lopez and in the whole eastern Tropical Atlantic Ocean. From the analysis of oceanic and atmospheric
20 conditions during this particular event, it appears that anomalous strong boreal spring wind strengthening
21 associated to anomalous strong Hadley cell activity prematurely triggered the rainfall coastal onset in the
22 northern Gulf of Guinea, making it the earliest over 1998-2008 period. Results show that no similar atmospheric
23 conditions were observed in May over the 1998-2008 period. It is also found that the anomalous oceanic and
24 atmospheric conditions associated to the event exerted strong influence on rainfall off Northeast Brazil. This
25 study highlights the different processes through which the wind power from South Atlantic is brought to the
26 ocean in the Gulf of Guinea and emphasizes the need to further document and monitor the South Atlantic
27 region.

28

29 **1.Introduction**

30 The eastern equatorial Atlantic Ocean shows a pronounced seasonal cycle in sea surface temperature (SST)
31 (Wauthy, 1983; Mitchell and Wallace, 1992). One strong signature of the SST seasonal cycle in the eastern
32 equatorial Atlantic is the Atlantic cold tongue (ACT) (Zebiak, 1993) characterized by a fast drop of SST (up to
33 7° C) in boreal spring and summer slightly south of the equator and east of 20°W (Merle, 1980; Picaut, 1983).

34 During boreal summer, the southern boundary of this cooler temperature connects progressively with the austral
35 winter cooling of the Southern hemisphere SSTs. A number of observational (Merle, 1980; Foltz et al., 2003)
36 and modeling (Philander and Pacanowski, 1986; Yu et al., 2006; Peter et al., 2006) studies show that the
37 development of the ACT is driven by the seasonal increase of the Southern Hemisphere trade winds during late
38 boreal winter to early summer (Brandt et al., 2011) **associated with** the meridional displacement of the Inter-
39 Tropical Convergence Zone (ITCZ) (Picaut, 1983; Colin, 1989; Waliser and Gautier, 1993; Nobre and Shukla,
40 1996). The equatorial cooling **is regulated** by a coupling between thermocline shoaling, subsurface dynamics
41 (Yu et al., 2006; Peter et al., 2006; Wade et al., 2011; Jouanno et al., 2011) including turbulent mixing, vertical
42 advection and entrainment, as well as horizontal advection. The equatorial thermocline shoaling is the
43 consequence of local and remote wind forcing: the strengthening of easterly winds in the western equatorial
44 Atlantic remotely forces the seasonal upwelling in the eastern part of the basin via equatorial Kelvin waves
45 (Moore et al., 1978; Adamec and O'Brien, 1978; Busalacchi and Picaut, 1983; McCreary et al., 1984).

46 Besides the dominant seasonal cycle, the eastern tropical Atlantic is under the influence of meridional southerly
47 winds (Picaut, 1984) which fluctuate with a period close to 15 days (Krishnamurti, 1980; de Coëtlogon et al.,
48 2010; Jouanno et al., 2013). These intraseasonal wind fluctuations are therefore expected to be a major
49 contributor to the seasonal SST cooling and **occur as an energy and momentum carrier** from the South Atlantic
50 to the eastern equatorial Atlantic. A connection between the strength of the St. Helena Anticyclone and SST
51 anomalies in the southeastern tropical Atlantic has been described by Lübbecke et al. (2014). These authors
52 suggest that the St. Helena Anticyclone variability might be an **important** source of anomalous tropical Atlantic
53 wind power which affects SST in the eastern equatorial Atlantic via several mechanisms: zonal wind stress
54 changes in the western equatorial basin, wave adjustment, meridional advection of subsurface temperature
55 anomalies, intraseasonal wind stress variations, and possibly even other mechanisms. Through the in situ data
56 analysis of AMMA/EGEE cruises (Redelsperger et al., 2006; Bourlès et al., 2007) carried out in 2005 and 2006,
57 Marin et al. (2009) show that the SST seasonal cooling at the equator east of 10° W is not smooth but results
58 from the succession of short-duration cooling episodes generated by southeasterly wind bursts due to the
59 fluctuating St. Helena Anticyclone. In addition, according to Leduc-Leballeur et al. (2013), the sharp and
60 durable change in the atmospheric circulation in the northern Gulf of Guinea (durably strong southerlies north of
61 equator) takes place through an abrupt seasonal transition prepared by a succession of southerly wind bursts and
62 possibly triggered by a significantly stronger wind burst. The southerly wind bursts occurring in boreal spring in
63 the Gulf of Guinea thus would play an important role in driving precipitation pattern in the area through air-sea
64 interactions (de Coëtlogon et al., 2010; Nicholson and Dezfuli, 2013) and coupling between the ACT and the
65 West Africa Monsoon (WAM).

66 Improving our understanding of the impact of such wind bursts on SST variability at intraseasonal scale in the
67 eastern Tropical Atlantic is important through its link with the regional climate. However, while the ACT and
68 Angola-Benguela regions have been the object of many studies, the dynamics and SST variability of the coastal
69 eastern region is much less documented.

70 In this study, we therefore first focus our analysis off Cape-Lopez (defined from 0° N-7° S; 5° E-14° E and
71 hereafter called CLR for ‘Cape-Lopez region’, see Fig. 2) and aim to improve understanding of its seasonal SST
72 variability and the impact of intraseasonal winds on SST variability during boreal spring and summer. To this
73 end, we use regional high resolution model results as well as satellite SST data and sea surface height
74 observations. We first use model outputs from 1998 to 2008 to analyze the seasonal cycle in CLR and to
75 highlight its interannual variability, and then we specially focus on the years 2005 and 2006 to investigate the
76 SST response of intraseasonal wind forcing. These two particular years were largely investigated during the
77 African Monsoon Multidisciplinary Analyses (AMMA) experiment (Redelsperger et al., 2006). The year 2005
78 is characterized by the lowest SST values in the ACT during the past 3 decades (along with 1982), while 2006 is
79 considered as a normal year (Caniaux et al., 2011). Also, 2005 exhibits the earliest development of the ACT.
80 The study of SST variability at intraseasonal scale during these two years is thus interesting for better
81 understanding their observed differences in SST seasonal conditions. These two particular years have been also
82 chosen by Marin et al. (2009) to study the variability of the properties of the ACT. Their study concerned the
83 equatorial area west of 4° E, whereas we propose to focus in CLR, east of 5° E where coastal processes are
84 expected to be involved.

85 The question of the processes implied in the SST variability in the Cape-Lopez region was raised based on an
86 observation in satellite SST data of cold coastal waters during boreal spring independent from those observed
87 off shore in the cold tongue region around 10°W (see Fig. 2) which also raised the question of the link of such
88 cooling with the cold tongue development. Most studies on the CLR focused on the analysis of observational
89 data sets to examine the hydrology and its seasonal variation along the frontal (coastal) region of Congo (e.g.
90 Merle, 1972; Piton, 1988) or on the impact of Congo River on SST and mixed layer (e.g. Matera et al., 2012;
91 Denamiel et al., 2013; White and Toumi, 2014) but, to our knowledge, no detailed analysis of SST variability at
92 seasonal and intraseasonal time scales have been realized. A better understanding of ocean-atmosphere
93 interactions in this region is thus needed. Some previous studies related to the whole eastern Tropical Atlantic
94 (Gulf of Guinea) suggest that multiple processes could be at play in the CLR, coupling remote and local forcing.
95 For example, Giordani et al. (2013) show from regional model results that horizontal advection, entrainment,
96 and turbulent mixing significantly contribute to the heat budget east of 3°W because of the very thin mixed
97 layer. The upper layers of the north CLR might also be impacted by vertical mixing induced by the intense
98 current vertical shear between the South Equatorial Current, flowing westward at the surface, and the subsurface
99 eastward Equatorial Under-Current. In addition to local forcing, the area is also under the influence of the arrival
100 of equatorial Kelvin waves from West and their reflection, once reaching the African coast, poleward as
101 coastally trapped waves and westward as Rossby waves (Moore, 1968; McCreary, 1976; Moore and Philander,
102 1977). The principal source of the equatorial Kelvin waves has been usually related to the western equatorial
103 zonal wind changes during late boreal winter to early summer (e.g.; Philander, 1990). In order to better
104 understand the trigger mechanism of Kelvin waves generation which conditions the mixed layer properties in
105 the CLR, another purpose of this study is thus to identify the atmospheric conditions coinciding with the Kelvin
106 waves generation in the West of the basin during winter 2005 and 2006. In addition, some studies (such as

107 DeCoëtlogon et al., 2010) suggest that at short time scale (a few days), more than half of the cold SST anomaly
108 around the equatorial cooling could be explained by horizontal oceanic advection of upwelled cold coastal
109 waters controlled by the winds. Therefore, a better understanding of the SST variability in the CLR may also
110 help to better understand the SST variability in the equatorial region.

111 Several studies (*e.g.* Okumura and Xie, 2004; Caniaux et al., 2011; Nguyen et al., 2011; Thorncroft et al., 2011)
112 show evidence of a high correlation between the ACT and the WAM onset in the Sahelian region. Based on an
113 analysis of 27 years of data, Caniaux et al. (2011) identified the year 2005 as the year with the earliest WAM
114 onset date (around 19 May 2005 whereas they define the mean onset date on 23 June \pm 8 days). According to
115 Marin et al. (2009), the time shift in the development of the ACT between 2005 and 2006 is related to a
116 particular wind burst event in mid-May 2005. This mid-May 2005 event therefore appears as exerting a strong
117 influence on the WAM. In a second part of the study, we thus focus on this particular wind event that preceded a
118 strong cold event in the far eastern Tropical Atlantic along with an early ACT development. We aim to describe
119 i) the atmospheric and oceanic conditions during this particular event; ii) to what extent it is involved in the
120 WAM system; and iii) which processes make it an exceptional event.

121 The remainder of the paper is organized as follows. In Sect. 2, the model and observational data used in this
122 study are described. The seasonal and interannual variability of SST, winds, currents, 20° C-isotherm depth and
123 sea surface heat flux in the CLR are analyzed in Sect. 3. The cooling episodes generated in response to southerly
124 wind bursts and the other forcing mechanisms implied in the CLR are investigated in details for the years 2005
125 and 2006 in Sect. 4. In Sect. 5, we focus our analysis on the unusual wind burst occurring in mid-May 2005.
126 Finally, the main results are summarized and discussed in Sect. 6.

127

128 **2. Model and data**

129 The numerical model used in this paper is the Regional Oceanic Modeling System (ROMS) (Shchepetkin and
130 McWilliams, 2005). The model configuration is the same as employed in Herbert et al. (2016), and the
131 following text is derived from there with minor modifications.

132 ROMS is a three-dimensional free surface, split-explicit ocean model which solves the Navier-Stokes primitive
133 equations following the Boussinesq and hydrostatic approximations. We used the ROMS version developed at
134 the Institut de Recherche pour le Développement (IRD) featuring a two-way nesting capability based on AGRIF
135 (Adaptative Grid Refinement In Fortran) (Debreu et al., 2012). The two-way capability allows interactions
136 between a large-scale (parent) configuration at lower resolution and a regional (child) configuration at high
137 resolution. The ROMSTOOLS package (Penven et al., 2008) is used for the design of the configuration. The
138 model configuration is built following the one performed by Djakouré et al. (2014) over the Tropical Atlantic.
139 The large scale domain extends from 60° W to 15.3° E and from 17° S to 8° N and the nested high resolution
140 zoom focuses between 17° S and 6.6° N and between 10° W and 14.1° E domain. This configuration allows for
141 equatorial Kelvin waves induced by trade wind variations in the western part of the basin to propagate into the

142 Gulf of Guinea and influence the coastal upwelling (Servain et al., 1982; Picaut, 1983). The horizontal grid
143 resolution is $1/5^\circ$ (i.e. 22 km) for the parent grid and $1/15^\circ$ (i.e. 7 km) for the child grid (see Herbert et al.
144 (2016), their Fig. 1). This allows an accurate resolution of the mesoscale dynamics since the first baroclinic
145 Rossby radius of deformation ranges from 150 to 230 km in the region (Chelton et al., 1998). The vertical
146 coordinate is discretized into 45 sigma levels with vertical S-coordinate surface and bottom stretching
147 parameters set respectively to $\theta_s = 6$ and $\theta_b = 0$, to keep a sufficient resolution near the surface
148 (Haidvogel and Beckmann, 1999). The vertical S-coordinate H_c parameter, which gives approximately the
149 transition depth between the horizontal surface levels and the bottom terrain following levels, is set to $H_c = 10$
150 m. The GEBCO1 (Global Earth Bathymetric Chart of the Oceans) is used for the topography (www.gebco.net).
151 The runoff forcing is provided from Dai and Trenberth's global monthly climatological run-off data set (Dai and
152 Trenberth, 2002). The rivers properties of salinity and temperature are prescribed as annual mean values. One
153 river (Amazon) is prescribed in the parent model while five rivers, that correspond to the major rivers present
154 around the Gulf of Guinea, are prescribed in the child model (Congo, Niger, Ogoou, Sanaga, Volta). At the
155 surface, the model is forced with the surface heat and freshwater fluxes as well as 6 hourly wind stress derived
156 from the Climate Forecast System Reanalysis (CFSR) (horizontal resolution of $1/4^\circ \times 1/4^\circ$) (Saha et al., 2010). Our
157 model has three open boundaries (North, South, and West) forced by temperature and salinity fields from the
158 Simple Ocean Data Analyses (SODA) (horizontal resolution of $1/2^\circ \times 1/2^\circ$) (Carton et al., 2000a, 2000b; Carton
159 and Giese, 2008). The simulation has been performed on IFREMER Caparmor super-computer and integrated
160 for 30 years from 1979 to 2008 with the outputs averaged every 2 days. A statistical equilibrium is reached after
161 ~ 10 years of spin-up. Model analyses are based on the 2-days averaged model outputs from year 1998 to year
162 2008. The model has already been validated successfully with a large set of measurements and climatological
163 data, and more detailed information about the model validations can be found in Herbert et al. (2016).
164 Note that throughout the whole text and figure captions, the term "intraseasonal variations" is used to designate
165 the field obtained after removing the 30 days low-pass filtered field to the total field of the given year, while
166 "intraseasonal anomaly" refers to the field obtained after removing the 30 days low-pass filtered field averaged
167 over 1998-2008 to the total field of the given year.
168
169 For SST observations, we use data obtained from measurements made by the Tropical Rainfall Measuring
170 Mission microwave imager (TMI). The dataset is a merged product available at www.remss.com. The SST data
171 have a spatial resolution of $1/4^\circ$ and for the present study the 10 years' time series, from 1 January 1998 to 31
172 December 2008, obtained as 3-daily field. The important feature of the microwave retrievals is that it can give
173 accurate SST measurements under clouds (Wentz et al., 2000). However, the major limitation to the microwave
174 TMI observations is land contamination which results in biases of the order of 0.6°K within about 100 km from
175 the coast (Gentemann et al., 2010). Thus, in the Optimal Interpolation TMI product the offshore zone with no
176 data extends at approximately 100 km from the coast. This limits to some degree the analysis of near-coastal
177 regions, in particular those dominated by coastal upwelling dynamics.

178 We also use for this study daily sea surface height (SSH) data, which are available for the period 1993–2012 and
179 maintained by the organization for Archiving, Validation, and Interpretation of Satellite Oceanographic data
180 (AVISO; www.aviso.altimetry.fr). The sea surface height dataset is a merged product of observations from
181 several satellite missions Ssalto/Duacs (Segment Sol multitemps d'ALTimétrie, d'Orbitographie et de
182 localisation précise/Developing Use of Altimetry for Climate Studies) mapped onto a 0.25° Mercator projection
183 grid. All standard corrections have been made to account for atmospheric (wet troposphere, dry troposphere and
184 ionosphere delays) and oceanographic (electromagnetic bias, ocean, load, solid Earth and pole tides) effects.
185 The mean sea surface topography for the period 1993–2012 was removed from the SSH to produce sea surface
186 height anomalies.

187 In addition, surface pressure data were studied using ECMWF Atmospheric Reanalysis (ERA) for the 20th
188 Century product. The four-hourly data are daily averaged and is available on <https://rda.ucar.edu> website. The
189 product assimilates surface pressure and marine wind observations.

190

191 **3. Seasonal variability of surface conditions in CLR**

192 The purpose of this section is to describe the seasonal atmospheric and ocean surface conditions in the CLR.

193 The seasonal variability of SST, surface winds stress, horizontal current intensity, depth of 20° C-isotherm
194 (hereafter referred to as z20), and the surface net heat flux from monthly averaged model outputs in the CLR for
195 each year from 1998 to 2008 and averaged over the period are shown in Fig. 1. The reliability of the model is
196 also provided by comparing the simulated and the corresponding TMI SST climatological seasonal cycle in the
197 CLR (Fig. 1a). The SST variations display an annual cycle with highest **temperature at the end of boreal winter**
198 **– beginning of boreal spring** (warm season), when the ITCZ reaches its southernmost position and the trade
199 winds are weakest, and minimum values in boreal summer (cold season), when the trades intensify. The most
200 salient features of the atmospheric and hydrographic fields during May-June are also illustrated in Fig. 1 by
201 May-June averaged maps. Despite a warm bias (~1°C) compared to satellite observations, the model **reproduces**
202 **the satellite pattern well**. While this warm bias in the eastern tropical Atlantic is well known in coupled climate
203 models (e.g. Zeng et al., 1996; Davey et al., 2002; Deser et al., 2006; Chang et al., 2007; Richter and Xie, 2008),
204 results from Large and Danabasoglu (2006) suggest indeed that a warm SST bias may also be present along the
205 Atlantic coast of southern Africa in forced ocean-only simulation. The SST May-June average map indicates
206 that the boreal summer SST minimum is related to intensified cool SST around 6°S, in the Congo mouth region.
207 In this region, the coast is oriented parallel to the trade flow which reinforces in boreal summer, thus favorable
208 to coastal upwelling processes. The mean alongshore wind stress during May-June reveals in fact that upwelling
209 conditions are observed over most of the CLR. **The coastal upwelling could also interact with the coastal Kelvin**
210 **wave propagation (e.g. Ostrowski et al., 2009) highlighted by minimum z20 values in Fig. 1d.**

211 Wind stress magnitude exhibits a semi-annual variability with a second maximum in October–December and a
212 weakening during July-September season (Fig. 1b). The strengthening of winds in boreal spring is associated

213 with a strengthening of mean current speed, particularly off Cape-Lopez between 2° S to 4° S and west of 8° E
214 in May-June (Fig. 1c). The orientation of surface current is mostly westward for the May-June season, while it is
215 northward from October to January (not shown). This general picture of surface circulation is consistent with
216 observations (Merle, 1972; Piton, 1988; Rouault et al., 2009).

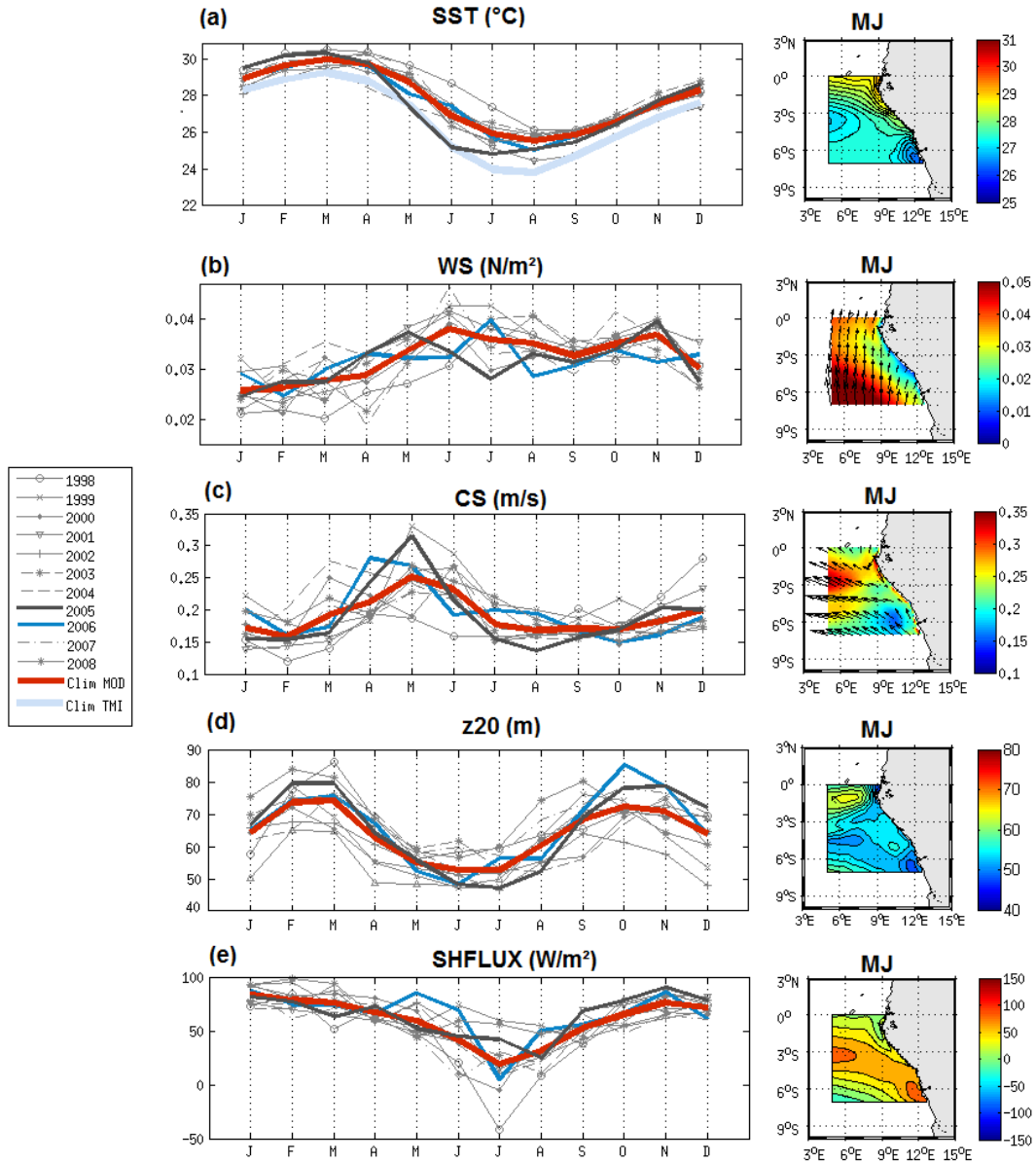
217 The region is also characterized by a shallow thermocline which depicts a strong semi-annual cycle (Fig. 1d).
218 The evolution of z20 reveals a shoaling of the thermocline during May-July and a deepening up to October-
219 November when it exhibits a maximum depth, in agreement with previous studies such as the one realized by
220 Schouten et al. (2005) who find a similar seasonal cycle from SSH altimetric data.

221 The surface net heat flux exhibits a maximum in boreal winter and a minimum in July (Fig. 1e), following the
222 seasonal cycle of solar shortwave radiations. As visible on the May-June average map, greater heating is found
223 over cool waters, due to weaker heat loss via latent heat flux in these areas.

224 The seasonal cycle is modulated by strong year-to-year variations. The mean SST in the CLR in 2005 cools as
225 early as March from TMI data and April from the model data. SST reaches **lower** values than the climatologic
226 ones, as observed by Marin et al. (2009) and Caniaux et al. (2011) west of 4° E. This 2005 cold anomaly is
227 associated with positive wind speed and surface current speed anomaly in April-May (Fig. 1b&c) as well as
228 shallower-than-average thermocline depth. In 2006, SST variations are very close to the climatologic ones.

229

230 Thus, the April-June season in the CLR appears as a transitional period characterized by strong seasonal
231 evolution, primarily governed by the local winds which generate coastal upwelling in Congo mouth region and
232 modulated by the variation of thermocline depth.



233

234 **Figure 1:** Monthly average of the (a) sea surface temperature ($^{\circ}\text{C}$); (b) wind stress direction (vectors) and
 235 magnitude (color field) ($\text{N}\cdot\text{m}^{-2}$); (c) horizontal surface current direction (vectors) and speed (color field) ($\text{m}\cdot\text{s}^{-1}$);
 236 (d) 20°C -isotherm depth (m); and (e) surface heat flux ($\text{W}\cdot\text{m}^{-2}$; positive values indicate downward flux) from
 237 January to December from 1998 to 2008 and for the climatology (averaged over 1998-2008) simulated by the
 238 model (red curve) and from the observations : monthly average TMI 3-daily SST data (light blue curve in (a));
 239 averaged over 5°E - 14°E and 7°S - 0°S . Right panel: maps of each variable over May-June..

240

241 **4. Analysis of cooling episodes in the CLR in 2005 and 2006**

242 In this section, we examine the impact of intraseasonal wind bursts on SST in the CLR during the particular
243 years 2005 and 2006 (Marin et al., 2009; Caniaux et al., 2011). We propose here to analyze in details the SST
244 conditions in CLR, east of 5° E, for both years.

245

246

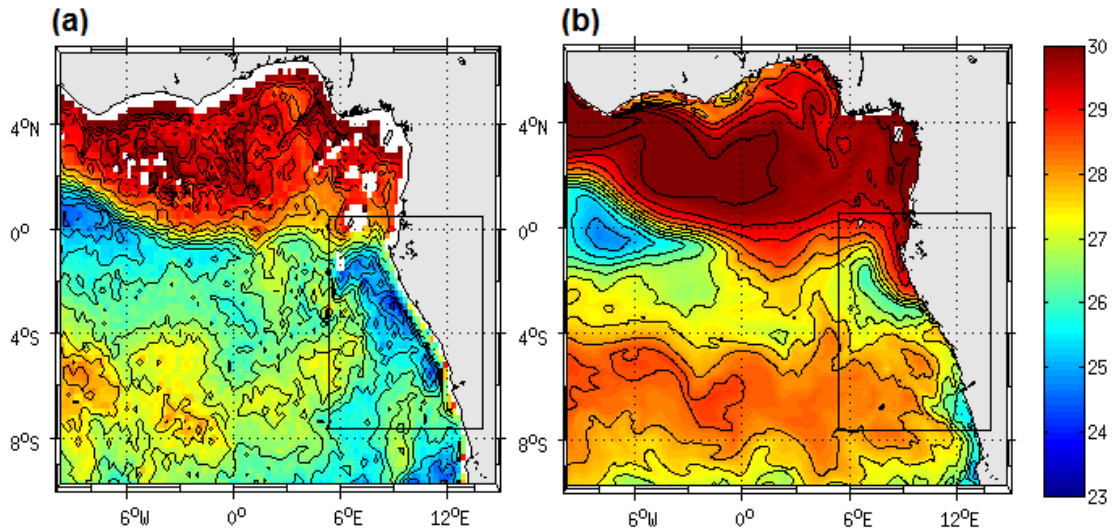
247 **4.1 SST variations**

248 In order to delineate the sequence of cooling episodes, we analyze the SST variations from 2-days averaged
249 model outputs in 2005 and 2006 over the CLR, i.e. between 5° E and 12° E. Both the SST (Fig. 3a & c) and
250 intraseasonal variations of SST (Fig. 4a & f) are shown. The cooling episodes occurred east of 5° E from April
251 to September. In 2005, the intraseasonal cooling episodes took place on 8-12 May, 16-22 May, 30 May-June 6,
252 and 12-16 June, whereas in 2006, they took place on 20-30 April, 14-24 May, 14-20 & 26-30 June. The
253 temperature drop for the two years ranged between -0.2°C to -2°C. The cooling episodes concerned especially
254 the southern equatorial region (around ~3-4° S), except for the strongest events where they reached more
255 northern equatorial regions, especially for the mid-May and late-May 2005 events. These latter were associated
256 with an intense meridional SST front between the cold water south of the equator and the warmer water north of
257 the equator, as visible on SST map for 12 May 2005 presented in Fig. 2. We can see cold waters extending
258 along the eastern coast and in ACT region west of 5° W. In the model, cold waters are deflected offshore off
259 Cape-Lopez, due to recursive bias in warm water intrusion toward the south.

260 Besides, model SST fields (Fig. 3a) indicate that the SST minimum (~24° C) in 2005 was reached in July, i.e.
261 one month earlier than in 2006, as also noticed in seasonal variations of SST averaged in the region (Fig. 1a).
262 These results illustrate the important role of the succession of quick and intense cooling episodes in the
263 establishment of persistent cold anomalies in the CLR, as highlighted by Marin et al. (2009) in the equatorial
264 region.

265

266



267

268 **Figure 2:** Map of the sea surface temperature ($^{\circ}$ C) on 12 May 2005 from 3-days average TMI data (a) and from
 269 the 2-days average model output (b). Note that for the model it corresponds to 11-12 May average whereas for
 270 TMI data it is 10-11-12 May average. The black square indicates the Cape-Lopez region (called ‘CLR’).

271

272 4.2 Forcing mechanisms

273 4.2.1. Local forcing

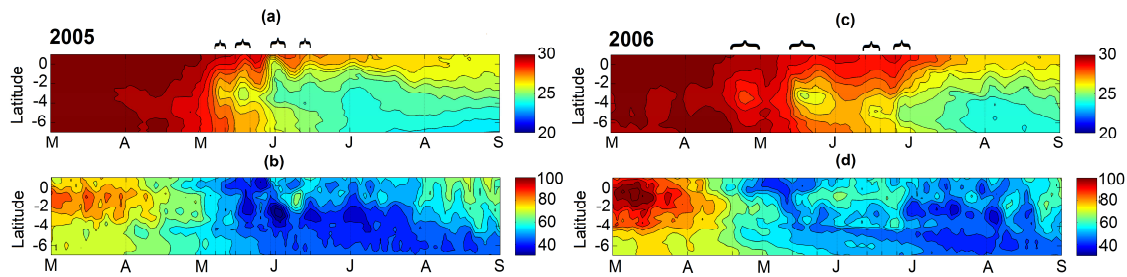
274 To examine the local forcing mechanisms responsible for the observed cooling episodes in CLR, the
 275 intraseasonal variations of wind stress magnitude are examined and compared in 2005 and 2006 (Fig. 4b & 4g).
 276 In 2005, successive periods of 6-16 days wind intensification occurred from late-March to late-June. The main
 277 cooling episodes described above are associated with positive intraseasonal wind stress speed occurring on **6-8,**
 278 **14-18 & 26-30 May, and 10-14 & 28 June-2 July with a maximum for the 14-18 May event peaking on 16 May**
 279 (at $\sim 0.025 \text{ N.m}^{-2}$). Another period of wind intensification is **evident** in late March – early April but it did not
 280 generate significant cooling despite comparable or even higher wind intensity than following wind events. In
 281 2006, periods of wind intensification extended from mid-March to July. The main wind events in boreal spring
 282 occurred **in 2-4 & 16-24 April, 6-8 & 14-20 May, 14-16 & 24-26 June** with maximum intraseasonal wind stress
 283 magnitude in 16-24 April (0.019 N.m^{-2}) and 24-26 June (0.022 N.m^{-2}). Also, the wind event in late April 2006
 284 did not generate a surface cooling as strong as the mid-May 2006 one, despite higher wind stress magnitude. To
 285 depict the subsurface conditions during cooling episodes in the CLR for both years, the 20° C-isotherm depths
 286 averaged from 5° E to 12° E are presented **in** Fig. 3b & 3d. They indicate strong correlation with SST variations
 287 on intraseasonal time scale with minimum depths ($< 35 \text{ m}$) observed during the mid-May 2005 and end-May
 288 event. In early April 2005 and before the late-April 2006, the thermocline was deeper, that can explain why
 289 wind intensification did not generate a surface cooling at these times. Indeed, at the time of the strong 16-24

290 April 2006 wind event, the z_{20} values was higher south of the equator than during the 14-16 May 2005 event,
291 making the SST less reactive to comparable wind intensification. The same feature is observed in early May
292 2006, when the higher z_{20} values indicate deeper thermocline south of the equator around 3-4° S than a few
293 days later. Besides, the thermocline appeared shallower south of the equator in 2005 than in 2006, in agreement
294 with the difference of the cooling intensity observed between the two years.

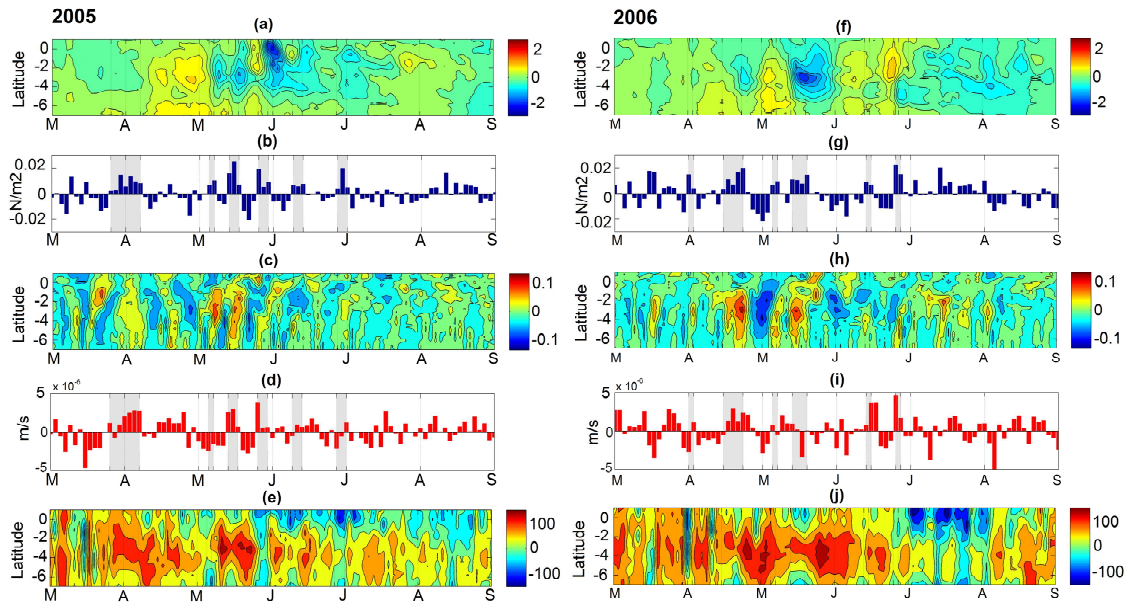
295 The Ekman pumping velocity w_e averaged over the CLR for 2005 and 2006 is shown in Fig. 4d & 4i
296 respectively. The dates of intraseasonal upward velocities are quite well correlated with the dates of
297 intraseasonal wind events (with correlation coefficient equal to 0.55 for 2005 and 0.41 for 2006), maximum
298 being during the early-April, mid-May and end-May 2005 events and during .late April, mid-June and end-June
299 2006. However, for comparable wind intensification, the boreal spring and summer wind events were not
300 associated with comparable intensity of Ekman pumping velocity.

301 Another process that may contribute to the cooling in the upper layer is the vertical mixing due to intense
302 vertical shear of the current. The maximum of the vertical shear magnitude fields in the CLR, averaged between
303 5° and 12° E for 2005 and 2006 (Fig. 4c & 4h), exhibited intensification south of the equator, centered around 3-
304 4° S. Weaker intensification also occurred occasionally at the equator (located around 80 m depth between the
305 westward surface South Equatorial Current – SEC – and the eastward subsurface Equatorial Under- Current).
306 Around 3-4°S, the vertical shear was driven by the SEC, reinforced by prevailing southerly winds events
307 through Ekman transport. It thus occurred at the date of wind events previously identified for 2005 and 2006,
308 with stronger vertical shear occurring in early May 2005 and late April 2006. The intensity of the maximum of
309 vertical shear magnitude during the events was quite similar between 2005 and 2006. The main difference lied
310 in their meridional extent, related to the meridional extent of the strengthened southerly winds which reached
311 equatorial region during the May 2005 events (not shown). We can also notice that for comparable wind
312 intensification, the boreal spring and summer wind events were not associated with comparable intensity of
313 vertical shear. The meridional wind component favorable to westward Ekman transport was actually stronger
314 during April and May events than during summer ones (not shown).

315 The heat content within the mixed layer is also impacted by the sea surface heat fluxes.
316 The net heat fluxes averaged between 5° E and 12° E are shown in Fig. 4e & 4j for 2005 and 2006 respectively.
317 They indicate a net heating ($\sim 50-100 \text{ W.m}^{-2}$) over the 2° S - 5° S latitude band, where the SST cooling was
318 strongest, suggesting other mechanisms involved. However, we notice some particular events during which the
319 net heat flux was negative over most of the region. A strong net cooling (-30 W.m^{-2}) occurred during the 26-28
320 May 2005 event. It was mainly due to a sudden decrease of incoming surface short wave radiation (drop of
321 about 80 W.m^{-2} in the CLR between 22 and 28 May; not shown) suggesting increased cloud cover. Another
322 strong net cooling occurred on 2 April 2006 with a mean value in the CLR reaching -95 W.m^{-2} . It is more sudden
323 than the end-May 2005's one, and was almost exclusively restricted to the CLR region with values reaching
324 locally -185 W.m^{-2} (not shown). For both events, the net cooling did not concern the equatorial region west of
325 0°W.



327
328 **Figure 3:** (a & c) Latitude-time diagram of the sea surface temperature (°C) averaged between 5°E and 12°E; (b
329 & d) Latitude-time diagram of the 20° C-isotherm depth (m) averaged between 5° E and 12° E; from 1st March
330 to 31 August 2005 (left panels) and 2006 (right panels). The cooling episodes are indicated by the black
331 brackets.



332
333 **Figure 4:** (a & f) Time-latitude diagram, from 7° S to 1° N, of the intraseasonal variations of sea surface
334 temperature (in ° C) averaged between 5° E and 12° E; (b & g) Time evolution of the intraseasonal variations of
335 wind stress amplitude ($N.m^{-2}$) averaged between 5° E and 12° E and between 3° S and 0° S; (c & h) Latitude-
336 time diagram of the intraseasonal variations of the maximum of the current vertical shear magnitude ($m.s^{-1}$)
337 averaged between 5° E and 12°E; (d & i) Longitude-time diagram of the intraseasonal variations of Ekman
338 Pumping ($m.s^{-1}$) averaged over the CLR. Ekman pumping values >0 indicate upwelling; (e & j) Latitude-time
339 diagram of the net heat flux ($W.m^{-2}$) averaged between 5° E and 12° E; from 1st March to 31 August 2005 (left
340 panels) and 2006 (right panels). For details about calculations of intraseasonal variations, see Sect. 2. The
341 intraseasonal southerly wind events are indicated by the shaded areas. Note that the cooling episodes occur few
342 days after the southerly wind events.

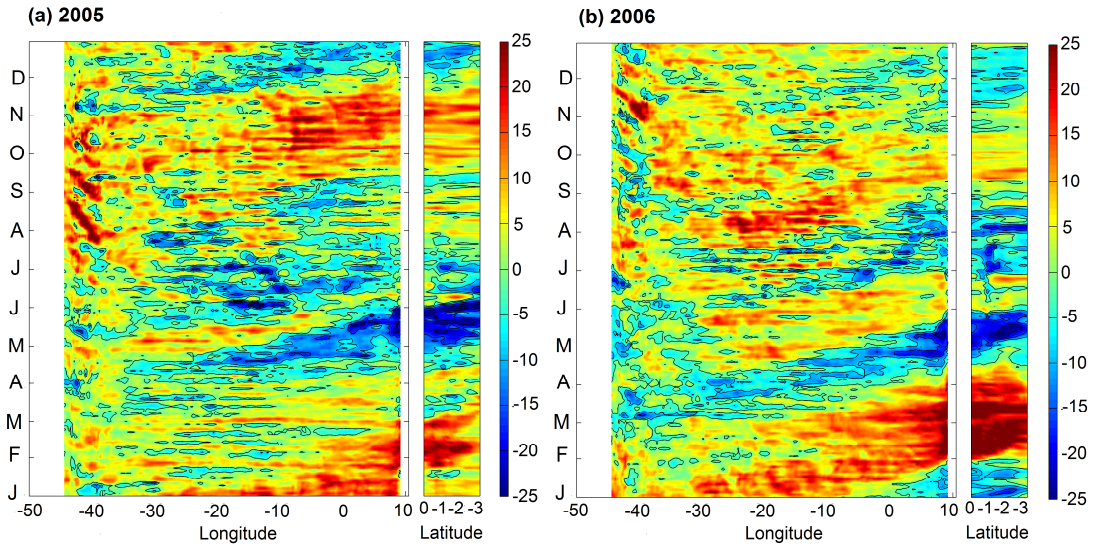
343 **4.2.2. Remote forcing**

344 **a. Highlighting of Kelvin wave propagation**

345 As previously shown, the time of occurrence of the cold events in the CLR coincides with shallow thermocline
346 **which contributes to making the mixed layer temperature more reactive to surface forcing (note that z20 is not**
347 **necessarily the same as the mixed layer depth).** Indeed, because of its proximity to the equator, the thermocline
348 in the CLR is affected by the arrival of equatorial waves, initiated in the western part of the basin. Pairs of
349 alternate downwelling and upwelling Kelvin waves occur usually in February-March, July-September and
350 October-November. Upon impingement with the eastern boundary, the incoming equatorial Kelvin wave excites
351 westward-propagating Rossby waves and poleward-propagating coastal Kelvin waves (Moore, 1968; Moore and
352 Philander, 1977; Illig et al., 2004; Schouten et al., 2005; Polo et al., 2008). The 20° C-isotherm depth anomalies
353 along the equator and along 9°E are presented in Fig. 5 and clearly evidence large negative anomalies indicating
354 shallower-than-average thermocline, propagating eastward along the equator and then southeastward for both
355 years. The eastward propagation of Kelvin wave along the equator and southeastward along the coast is also
356 well visible in the basin-wide SSH anomalies (Fig. 6) with a phase velocity of about 1.1-1.3m.s⁻¹, which fits
357 well in the range between the second and third baroclinic equatorial Kelvin wave modes. In 2005, negative SSH
358 and z20 anomalies occurred in the West in early March- early April and in mid-May, whereas they occurred
359 around late-February – mid-March and early May and June in 2006. The first Kelvin wave thus reached the
360 CLR slightly earlier in 2006 than 2005, at the beginning of May. In addition, the two upwelling Kelvin waves
361 followed each other more closely in 2005 than in 2006.

362 Thus, the intensity of the cold events observed in boreal spring and summer 2005 and 2006 resulted from both
363 the basin preconditioning by remotely forced shoaling of the thermocline, local mixing and upwelling processes
364 in response to strong southerly local winds, as well as heat flux variations. In 2005, stronger wind intensification
365 and favorably preconditioned oceanic subsurface conditions, made the coupling between surface and subsurface
366 ocean processes more efficient than in 2006, resulting in stronger cooling.

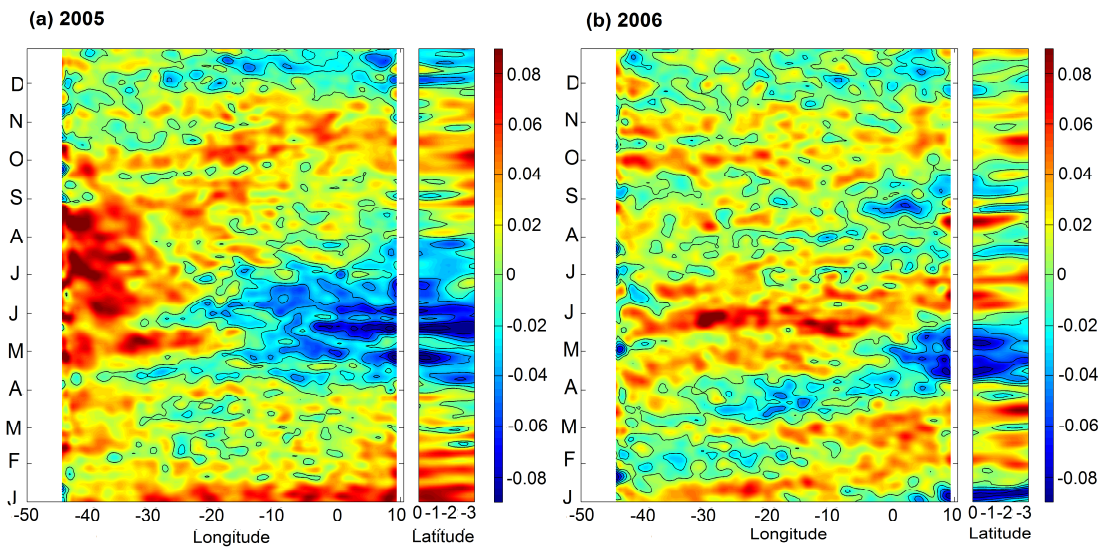
367



368

369 **Figure 5:** Time evolution of the intraseasonal anomaly of 20° C-isotherm depth (m) along the equator (between
 370 54° W and 12° E) and along 9° E (between the equator and 3° S) for 2005 (left) and 2006 (right). Negative
 371 values indicate a 20°C isotherm depth closer to the surface. For details about calculations of the anomalies, see
 372 Sect. 2.

373



374

375 **Figure 6:** Time evolution of the sea level anomaly (m) along the equator (between 54° W and 12° E) and along
 376 9° E (between the equator and 3° S) for 2005 (left), and 2006 (right) from AVISO data.

377

378

379 **b. Kelvin wave generation and coinciding atmospheric conditions in the West**

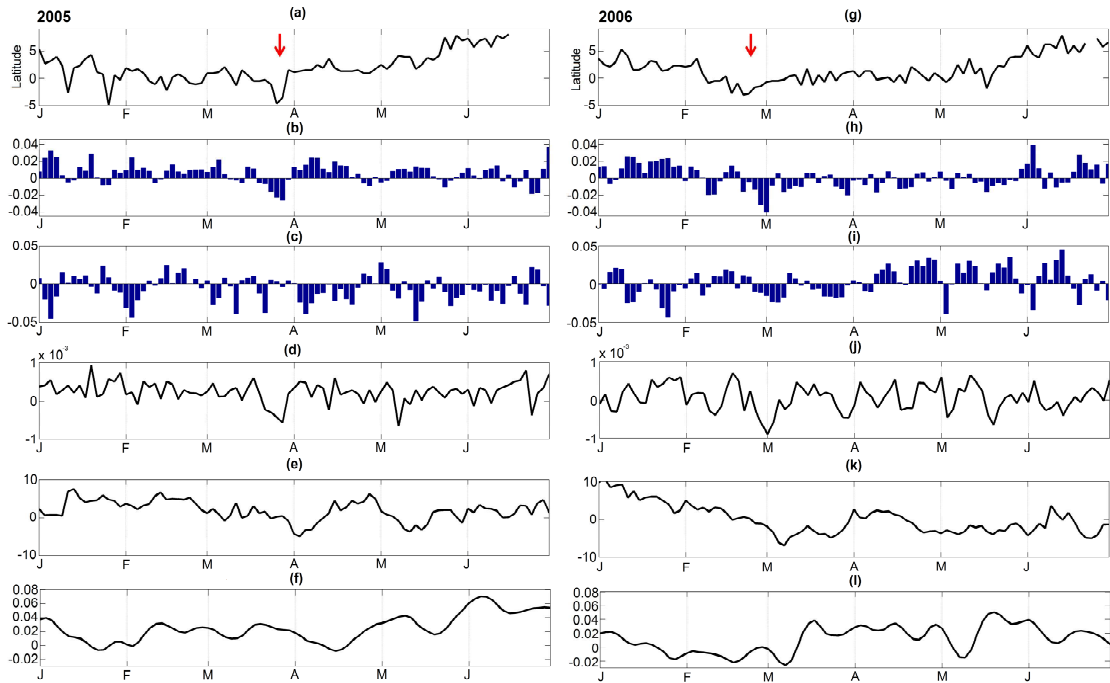
380 In order to identify the wind activity which accompanies the generation of Kelvin upwelling waves in winter
381 2005 and 2006 in the western part of the basin, we analyze the position of the ITCZ (averaged over 50° W-35°
382 W) identified as the latitude where the meridional wind stress goes to zero (Fig. 7a & g). The intraseasonal
383 anomaly of the zonal and meridional components of the wind stress (Fig. 7b-c & 7h-i), the intraseasonal
384 anomaly of wind stress curl (Fig. 7d & j), as well as the intraseasonal anomaly of the z20 and SSH (Fig. 7e-f &
385 k-l), averaged in the equatorial band (over 1° S and 1° N), are also presented. Many authors suggest that the
386 source of the equatorial Kelvin wave is mainly related to a sudden change of the western equatorial zonal wind
387 (e.g. Picaut, 1983; Philander, 1990): a symmetric westerly (easterly) wind burst along the equator will generate
388 Ekman convergence (divergence) and thus force downwelling (upwelling) anomalies which then propagate
389 eastward as a Kelvin wave (Battisti, 1988; Giese and Harrison, 1990). In 2005, shallower-than-average
390 thermocline, evidenced by negative z20 and SSH anomalies, occurred in the end of March-beginning of April in
391 the west part of the basin (Fig. 7e & f). The intraseasonal anomalies of meridional and zonal wind stress indicate
392 that the maximum of thermocline slope anomaly was associated with a strengthening of northeast trades
393 followed by a strengthening of southeast trades from either side on the equator. At the equator, we notice indeed
394 a sudden reversing of meridional winds which turned southward on 27-28 March 2005 related to an abrupt
395 southward displacement of the ITCZ which was then found south of the equator in the west part of the basin
396 (Fig. 7a & b). The ITCZ returned its initial position four days later followed by a strengthening of easterlies
397 which persisted for ~20 days (Fig. 7c). Climatologically, the latitudinal position of the ITCZ varies from a
398 minimum close to the equator in boreal spring (March-May) in the west to a maximum extension of 10°N –
399 15°N in late boreal summer (August) in the east. Positive (negative) wind stress curl is found north (south) of the
400 ITCZ. When the ITCZ is north of the equator, it induces upward (downward) Ekman pumping to the north
401 (south) of the ITCZ. Thus, the southward shift of the ITCZ on 27-28 March 2005 accompanied with strong
402 northerlies led to negative anomaly of wind stress curl south of the equator resulting in upward Ekman pumping.
403 Results show indeed a strong negative anomaly on 22-26 March 2005 associated with the southward shift of the
404 ITCZ just before the upwelling signal, initiated on 28 March. These changes contributed to a rise in the oceanic
405 thermocline with a time lag of some days (Fig. 7e & f). The upwelling signal might then be reinforced by the
406 symmetric easterly wind which concerned a large part of the western basin. Besides, we identify in Fig. 7d
407 another peak of negative wind stress curl anomaly on 6-8 May 2005, more sudden than the previous winter one.
408 It was associated with negative z20 SSH anomalies indicator of a thermocline rise initiated on 6 May 2005 in
409 the west of the basin and which propagated eastward along the equator. The zonal wind stress anomalies (Fig.
410 7c) also indicate an easterly wind strengthening initiated in the beginning of May, which a maximum on 8-10
411 May, just after the minimum of wind stress curl.

412 In 2006, the upwelling Kelvin wave is identified in the first half of March in the west part of the basin (Fig. 7k
413 & l). The coinciding atmospheric conditions were slightly different than the ones identified in 2005. In winter,
414 the position of the ITCZ had a more southern position in 2006 than in 2005. It crossed the equator during a
415 longer period (about 10 days from ~ Feb. 10 2006), reaching minimum latitude on 22-24 February. This location

416 south of the equator induced a negative wind stress curl anomaly (Fig. 7j). As in 2005, the reversion of the
 417 meridional wind at the equator was followed by a strengthening of westward component of the wind stress few
 418 days after, which lasted for about ten days (Fig. 7i); however, it was of a lesser magnitude compared to 2005
 419 and only concerned the westernmost part of the basin. In addition, the negative zonal wind anomaly concerned
 420 mainly the northeasterlies rather than the southeasterlies, leading to an anti-symmetric meridional wind pattern as
 421 well as symmetric zonal wind pattern on either side on the equator (not shown). These wind patterns were
 422 expected to generate **Ekman divergence** at the Equator and thus to reinforce the observed upwelling anomalies.

423

424 Thus, for both years, **upwelling Kelvin waves** were generated in the west while easterly winds were
 425 strengthened from either side of the equator after the ITCZ reached its southernmost location. This latter was
 426 observed one month earlier in 2006 than in 2005, and was associated with a negative wind stress curl anomaly.
 427 In winter 2005, the ITCZ was found south of the equator after a very sudden southward shift and was followed
 428 by strong easterlies during ~20 days, while in winter 2006, the ITCZ was found closer to the equator less
 429 sharply and during a longer period, followed by weaker easterlies compared to 2005. These results highlight
 430 another way in which **intraseasonal wind events** may impact the SST variability in the **eastern part** of the basin,
 431 through the generation of Kelvin wave in the West which shoals the thermocline in the East **a few weeks** later.



432

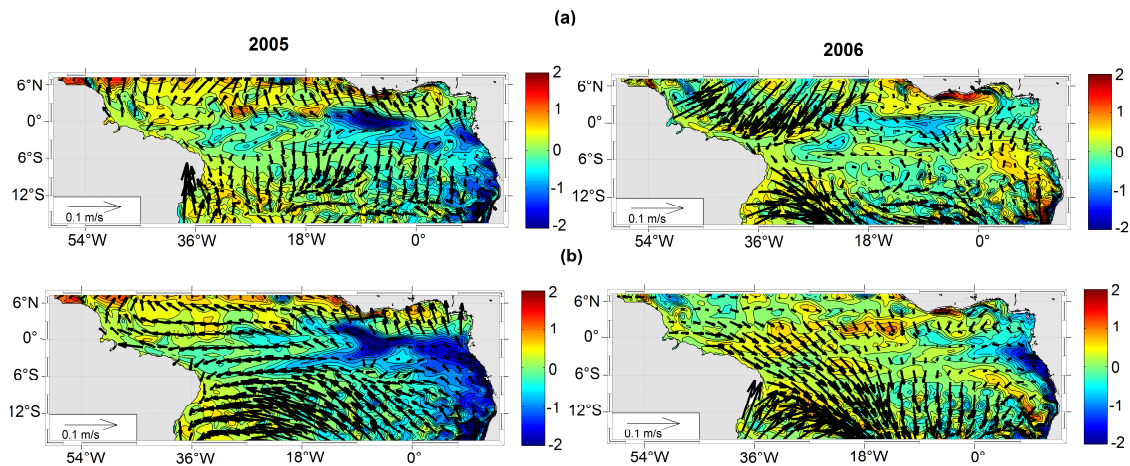
433 Figure 7: Time evolution, from 2-days averaged model outputs over Jan-June2005 (left) and Jan-June 2006
 434 (right); of (a & g) the position (in latitude, between 5° S and 10° N) where the meridional wind stress value
 435 equal zero (indicator of the position of the ITCZ); (b & h) the intraseasonal anomaly of the meridional wind
 436 stress ($N.m^{-2}$) averaged between 50° W and 35° W and between 1° S and 1° N; (c & i) same as (b & h) but for

437 intraseasonal anomaly of zonal wind stress ($\text{N}\cdot\text{m}^{-2}$); (d & j) the intraseasonal anomaly of the wind stress curl
 438 ($\text{N}\cdot\text{m}^{-2}$) ; (e & k) the intraseasonal anomaly of the 20°C isotherm depth (m); **negative values indicate that the**
 439 **20°C isotherm depth is closer to the surface** ; (f & l) the intraseasonal anomaly of the sea level (m). The red
 440 arrow in (a & g) indicates the southward shift of the ITCZ before the generation of the Kevin wave (see text).
 441 For details about the calculations of anomalies, see Sect. 2.

442

443 4.3. Westward extension of the CLR cooling

444 In the east, the cooling generated by southerly wind bursts in the CLR then progressively extended westward to
 445 connect with the southern boundary of the equatorial ACT. This phenomenon was more obvious in 2005 when
 446 the cooling which first concerned **the coastal area** extended further offshore a few days after the two strong
 447 events occurring in the second half of May. To evidence the effect of these events on SST, maps of
 448 intraseasonal SST anomaly and intraseasonal wind stress anomaly averaged from 1 to 12 May (before the strong
 449 2005 events; Fig. 8a) and from 14 to 31 May (during and after the strong 2005 events; Fig. 8b) are presented in
 450 Fig. 8. The same calculations **have been made** for 2006 for comparison. The results illustrate an enhancement
 451 after 10 May of the cooling in the east associated with southerly wind intensification and an extension of the
 452 cooling especially south of the equator up to 20°W .



453

454 **Figure 8:** (a) intraseasonal anomaly of sea surface temperature ($^\circ\text{C}$; color) superimposed with intraseasonal
 455 anomaly of wind stress intensity (arrows) averaged over 1-12 May 2005 (up panel) and over 14-30May (down
 456 panel); (b) same but for 2006. For details about the calculations of the anomalies, see Sect.2.

457 To better understand the oceanic processes implied in this cooling extension, we compared the SST, z_{20} , SLA
 458 and zonal velocities along 3°S from March to September 2005 (Fig. 9 a-d) and 2006 (Fig. 9 e-h). In 2005, the
 459 cooling westward extension was associated with a westward propagation of a shallower thermocline and
 460 negative SLA from the African coast up to 5° - 10°W combined with enhanced surface westward current

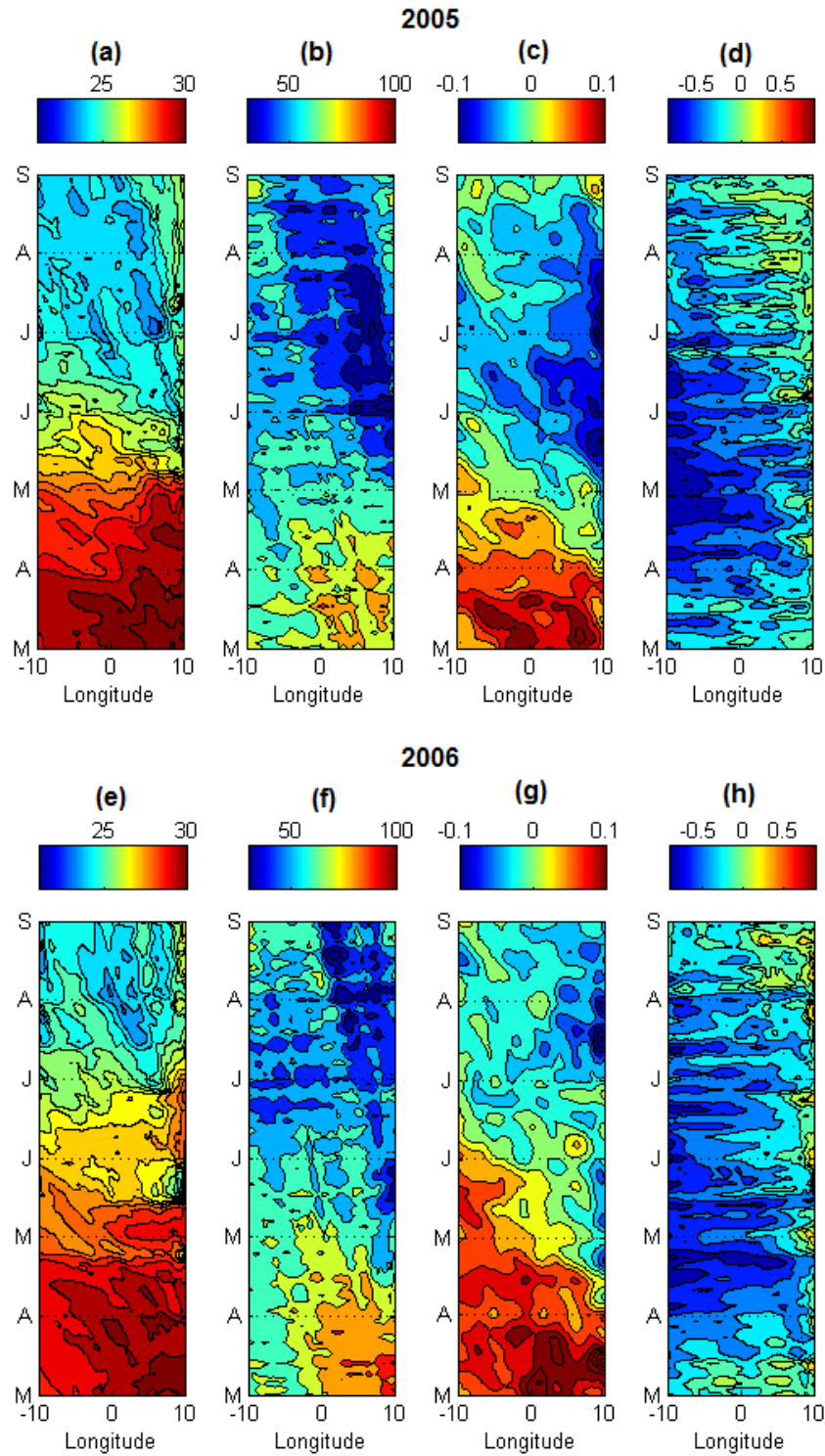
461 fluctuations at the dates of the successive events from April-June. The fluctuations of the westward surface
462 current occurring off Gabon with periods of ~8-10 days were related to the strengthening of southerly winds
463 during the wind bursts at the same periods (Fig. 4b & g). The surface current in this area is part of the westward
464 SEC which is known to intensify during the cold season (Okumura and Xie, 2006). Our study implies shorter
465 time scales than seasonal scale but the intensification of the SEC during wind bursts through Ekman transport
466 processes might contribute to the westward extension of the cooling by advection of cold eastern upwelled
467 water. This is in agreement with DeCoëtlogon et al. (2010) who found from model results that at short time
468 scale (a few days), more than half of the cold SST anomaly around the equatorial cooling could be explained by
469 horizontal oceanic advection controlled by the wind with a lag of a few days. In addition, minimum z20 and
470 SLA values propagating westward at 3° S (Fig. 9b & c), initiated from the coast with a propagating speed of
471 around 10 cm.s⁻¹, which is very close to the phase speed of Rossby waves. Indeed, the generation of the
472 westward waves at the coast coincided with the arrival of Kelvin waves (see Fig. 5a) suggesting the possibility
473 of Kelvin wave's reflection processes into symmetrical westward propagating Rossby waves. A westward
474 propagation of z20 and SLA minimums, although less obvious, was presently also identified at 3° N (not
475 shown).

476 In 2005, the locally wind-forced component of the wave might reinforce the remote part of the reflected wave
477 signal at the coast by the sea level slope which balanced the strengthening of alongshore winds blowing during
478 the mid-May and late-May events. The quantitative and respective contributions of local and remote wind
479 forcing to this wave is out of the scope of this study and would require further analysis. This phenomenon is
480 supported in 2005 by anomalous eastward expanded southerly wind bursts observed in May 2005. The month of
481 May is also a period when westward surface currents are usually maximum (as visible on the mean seasonal
482 cycle shown in Fig.1c). Thus, the combined effects of westward surface currents (via advection and vertical
483 mixing through horizontal current vertical shear), local wind influences (via vertical mixing) and wave
484 westward propagation, resulted in the extension of cold upwelled water from the eastern coast to near 20° W.

485 In 2006, the westward extension of cold waters established later, from the beginning of July. A coastal cooling
486 occurred on 18-26 May but no westward extension of the cold waters is observed at this period (Fig. 9e). In
487 2005, the two upwelling Kelvin waves followed each other closely while in 2006, the first Kelvin upwelling
488 wave reached the coast in May and the second in July (Fig.5b & Fig. 6b and Fig. 9f). In addition, the
489 intraseasonal wind strengthening responsible of the coastal cooling on 18-26 May 2006 is less intense (wind
490 stress mean in the CLR ~0.04N.m²) than the one in mid-May 2005 (~0.06N.m²; which is preceded and followed
491 by another wind bursts few days before and after; Fig. 3b & Fig. 4b).

492 The analysis over 1998-2008 period shows that the westward extension of the cold SST takes place every year
493 but begins at different times of the year (not shown). It occurs generally from June-July, when the cooling
494 events usually occur in the east at this location, and is thus closely linked with the shoaling of the thermocline
495 due to the arrival of a Kelvin upwelling wave at the eastern coast

496



497

498 **Figure 9:** Time-longitude diagrams at 3° S between 10° W and 10° E, and from 2-days averaged model outputs from 1st
 499 March to 31 August 2005 and 2006, of (a & e) the sea surface temperature (° C); (b & f) the 20° C isotherm-depth (m); (c &
 500 g) the sea level anomalies from AVISO data (m); and (d & h) the zonal component of surface velocity (m.s⁻¹).

501

502 In conclusion to this section 4, the SST variability in the CLR at intraseasonal time scales is the result of
503 combination between basin preconditioning by remotely forced shoaling of the thermocline via Kelvin wave,
504 local mixing induced by current vertical shear, and upwelling processes in response to strong southerly winds.
505 As highlighted for the 26-28 May 2005 and 2 April 2006 events, the net heat flux may also contribute to cool
506 the surface waters, through enhanced cloud cover which decrease the incoming solar radiation. The cold
507 upwelled waters around 3°S extend then westward from the eastern coast to near 20°W by combined effect of
508 the westward propagating Rossby waves as well as vertical mixing and advection processes. The cool water may
509 thus contribute to the cooling in the southern edge of the cold tongue region. Although the processes implied
510 differ slightly due to the presence of the coast, the SST variability in the CLR is quite close to the one in the
511 equatorial cold tongue region (not shown), due to similar atmospheric forcing. However, for a given wind burst,
512 the intensity of SST response in the CLR and in the cold tongue region is modulated by subsurface conditions
513 which are under the influence of equatorial Kelvin wave. In May 2005, the Kelvin wave reached the eastern
514 coast while three wind bursts occurred. The thermocline was thus shallower in the east than west of 0°W,
515 providing favorable subsurface conditions making the coupling between making the SST more reactive to wind
516 intensification occurred during this month. In addition, the decrease short wave radiations due to enhanced cloud
517 cover during the 26-28 May 2005 event or 2 April 2006 event, which contribute to the cooling in the CLR, did
518 not concern the equatorial region east of 0°W.

519

520 **5. Focus on the mid-May 2005 event**

521 We have previously identified five main cold events in 2005 (22-24 April, 8-12 May, 16-20 May, 26-30 May
522 and 14-18 June), characterized by a temperature drop ranging from -0.2° C to -1.7° C in the model. Analysis of
523 intraseasonal wind stress magnitude (Fig. 4b) has revealed that each event is associated with strengthening of
524 equatorward winds, especially during the 14-16 May event when the intraseasonal wind stress magnitude
525 averaged over the CLR is the strongest one. This particular event has been found to be responsible for the
526 sudden and intense SST cooling in the eastern equatorial Atlantic and identified as part of manifestation of
527 temporal variability of the St. Helena Anticyclone (Marin et al., 2009). In this section, we focus on this mid-
528 May event, to better understand the processes **at play** during this unusual event.

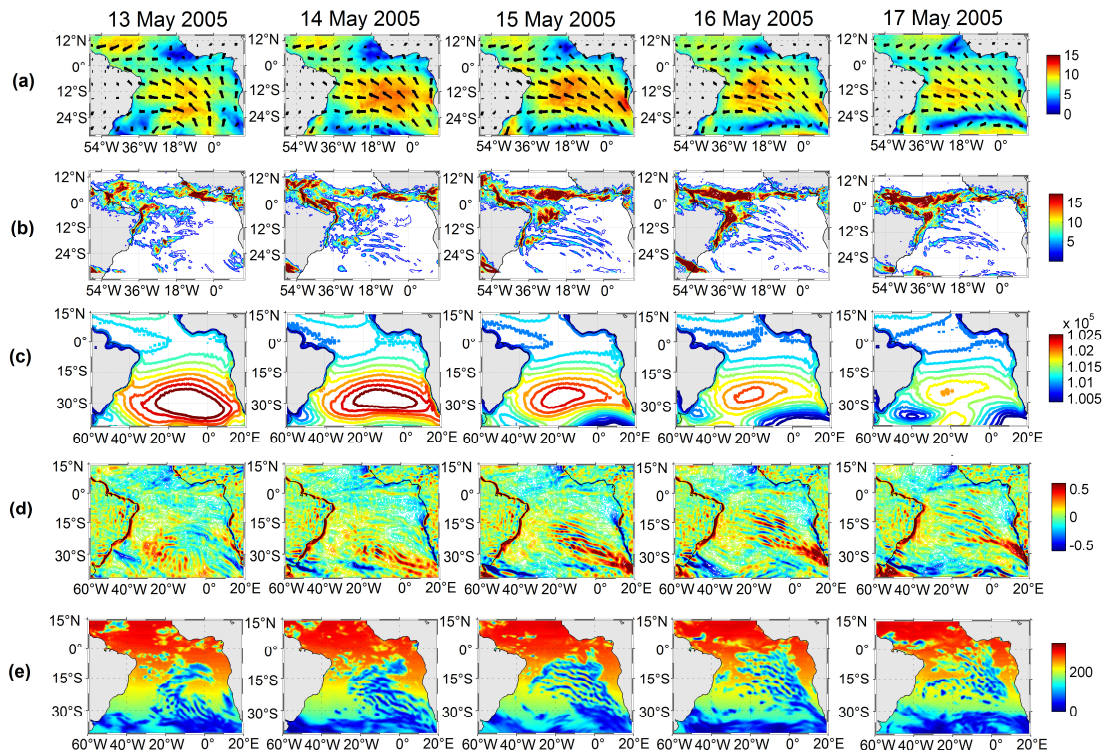
529 **5.1 Atmospheric conditions**

530

531 **5.1.1 Wind and surface atmospheric pressure**

532 The spatial distribution of the mid-May 2005 wind event can be inferred from Fig. 10 where CFSR wind speed
533 fields superimposed with daily precipitation fields, surface pressure, wind speed curl, and downward shortwave
534 radiation, are presented from 13 May to 17 May. The event was characterized by intense southeasterly wind east
535 of 15° W and from 30°S to the equator from 13-14 May, concomitant with a strengthening of the easterlies west

536 of 30° W between 30° and 15° S (Fig. 10a). The strong southeasterly winds drifted then westward up to 15-16
 537 May when the maximum was located in the western part of the basin off northeastern Brazilian coast.
 538 Simultaneously, a strengthening of southerly winds occurred north of the equator in the Gulf of Guinea. The
 539 strong winds during the event were associated with high pressure core of the Saint Helena Anticyclone,
 540 especially on 13-14 May, also associated with particularly low pressure under the ITCZ 4 days later (Fig. 10c).
 541 The pressure fall during the mid-May 2005 event appeared as the lowest in May over the whole decade (not
 542 shown). The meridional surface pressure gradient during the event is thus found to be the strongest over 1998-
 543 2008 period. That suggests strong Hadley circulation intensity during the mid-May event and therefore strong
 544 equatorward moisture flux, allowing the deep atmospheric convection in the Gulf of Guinea to be triggered at a
 545 self-sustaining level (see Sect. 5.2 following).



546

547 **Figure 10:** Daily-averaged, from 13 May to 17 May 2005 (left to right panels), of (a) wind magnitude (color
 548 field) (m.s^{-1}) superimposed with wind vectors from CFSR fields; (b) precipitation rate ($\text{kg.m}^{-2}/\text{day}^{-1}$) from
 549 CFSR fields; (b) surface pressure (hPa) from ERA-20C reanalysis; (c) wind speed curl (m.s^{-1}) computed from
 550 CFSR wind speed fields; and (d) downward short-wave radiation (W.m^{-2}) from CFSR fields.

551 **5.1.2 Precipitation**

552

553 The maps of precipitation rate during the event (Fig. 10b) display a band of heavy precipitation ($9\text{-}17 \text{ kg.m}^{-2}/\text{day}$)
 554 $^2/\text{day}$) between 5° - 9° N and off northeast Brazil from the coast to 15° W and from 10° S to 3° S. The maximum

555 precipitation rate in this region occurred on 15-16 May concomitant with the easterly winds strengthening. This
556 convective zone, located between the ITCZ north of the equator and the South Atlantic Convergence Zone
557 (SACZ) in southern tropics, is the Southern Intertropical Convergence Zone (SICZ) (Grodsky and Carton,
558 2003). This zone forms usually later, by June-August, when the southern branch of the convection separates
559 from the ITCZ which moves north of the equator. Grodsky and Carton (2003) showed that this rainfall pattern
560 appears closely linked to the seasonal change in SST difference between the ACT region (which they defined
561 between 15° W – 5° W, 2° S – 2° N) and the SITCZ region (25° W - 20° W, 10° S - 3° S). They argued that the
562 seasonal appearance of the ACT along the equator sets up pressure gradients within the boundary layer that
563 induce wind convergence in the SITCZ region. Based on Grodsky and Carton (2003) results, the unusually
564 rainfall conditions during mid-May event might thus be explained by strong SST gradient between the two
565 regions caused by unusually early cooling in the ACT region at this time of the year.

566

567 **5.1.3 Generation of atmospheric gravity wave**

568

569 The precipitation fields during the mid-May event (Fig. 10b) also evidence rainfall pattern typical of
570 atmospheric gravity wave train characterized by a horizontal wave length ~500 km and initiated by a front
571 system (forming the northern boundary of a low pressure system) which developed around 17° S on 14 May and
572 traveled northeastward until 17 May. The rainfall train was associated with oscillatory wind speed curl train
573 alternating between positive and negative values (Fig. 10d) as well as alternating downward shortwave radiation
574 minimum (Fig. 10e) associated with the wave clouds. Gravity waves are known to play an important role in
575 transporting the momentum and energy through long distances (Fritts, 1984). Here, they would be a way to
576 carry momentum and energy from South Atlantic to the equator during the strong event.

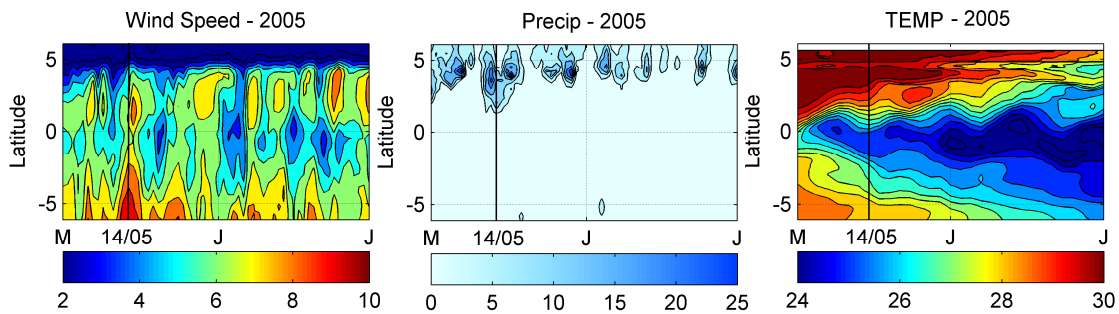
577

578 **5.2 A decisive event for coastal monsoon onset**

579 The mid-May 2005 wind event was found to be involved in the early onset of the ACT development (Marin et
580 al. 2009, Caniaux et al., 2011). The influence of the cold tongue on the WAM onset has been suggested by
581 several authors (Okumura and Xie, 2004; Caniaux et al., 2011; Nguyen et al., 2011; Thorncroft et al., 2011). At
582 the seasonal time-scale, Caniaux et al. (2011) suggest that it comes from strong interactions between the SST
583 cooling and wind pattern in the eastern equatorial Atlantic: the ACT serves to accelerate (decelerate) winds in
584 the northern (southern) hemisphere contributing to the northward migration of humidity and convection, and
585 pushes precipitation to the continent. Thus, due to its impact on ACT development, the mid-May 2005 wind
586 event is also linked to the onset of the WAM in 2005 which has been the earliest over 1982-2007 period from
587 Caniaux et al. (2011). In this section we aim to better understand how this single wind event may have such
588 impact. For further information on the WAM, the reader can refer to Leduc-Leballeur et al. (2013) and Caniaux
589 et al. (2011).

590

591 In order to analyze the air-sea pattern in the northern Gulf of Guinea during May-June 2005, we show in Fig. 11
 592 the wind magnitude, precipitation rate, and SST fields averaged from 10° W to 6° W. The wind strengthening
 593 appeared first south of the equator on 12-16 May and then north of the equator from 14-18 May. It was
 594 associated with strong rainfall extending southward up to 2° N. Equatorial cooling occurred 4 days after the
 595 event and slowed down the overlying winds by feedback mechanisms. The winds north of the equator then
 596 remained stronger than in the ACT region and strengthened again north of the Equator on 22-28 May together
 597 with precipitation maximum pushed northward (around 5° N) after the event.
 598 Thus, this mid-May event appears as the “decisive event” which triggered the abrupt transition between the two
 599 wind patterns in the northern Gulf of Guinea, when the wind north of the equator became and remained stronger
 600 than south of the equator. It occurred 15 days earlier than the average date (31 May) identified by Leduc-
 601 Leballeur et al. (2013) over 2000-2009 period. According to these authors, the time of occurrence of this
 602 phenomenon would be related with the strength of anomalous moisture flux. They explain that in April-May the
 603 low atmospheric local circulation is present only during an equatorial SST cooling and surface wind
 604 strengthening north of the equator, both generated by a southerly wind burst, before disappearing until the next
 605 wind burst. In June-July the low atmospheric local circulation is then always present and intensified by the wind
 606 bursts. Thus, the establishment of an abrupt seasonal transition event as observed in 2005, occurring much
 607 earlier than the reference date, supposed anomalously strong equatorial cooling caused by unusual strong
 608 southerly winds which allowed, through air-sea interactions mechanisms, to trigger the deep atmospheric
 609 convection in the Gulf of Guinea at a self sustaining level.



610
 611 **Figure 11:** Time evolution, in May and June 2005 between 6° S and 6° N and averaged between 10° W and 6°
 612 W, of the (a) daily averaged **wind magnitude ($m.s^{-1}$)** from CFSR wind fields ; (b) daily averaged precipitation
 613 rate ($kg.m^{-2}/day$) from CFSR fields and (c) 2-daily averaged SST ($^{\circ}C$) fields, from the forced model.

614

615 **5.3. What made the mid-May 2005 event so special?**

616

617 To better understand which makes the particularity of the mid-May 2005 event, the atmospheric and oceanic
 618 conditions (SST, intraseasonal SST anomalies, intraseasonal short-wave radiation flux anomalies (hereafter
 619 RADSW), intraseasonal wind stress magnitude anomalies, intraseasonal z20 anomalies, and intraseasonal
 620 meridional SST gradient anomalies) averaged over the 10° W - 6° W region and between 15° S to 5° N during

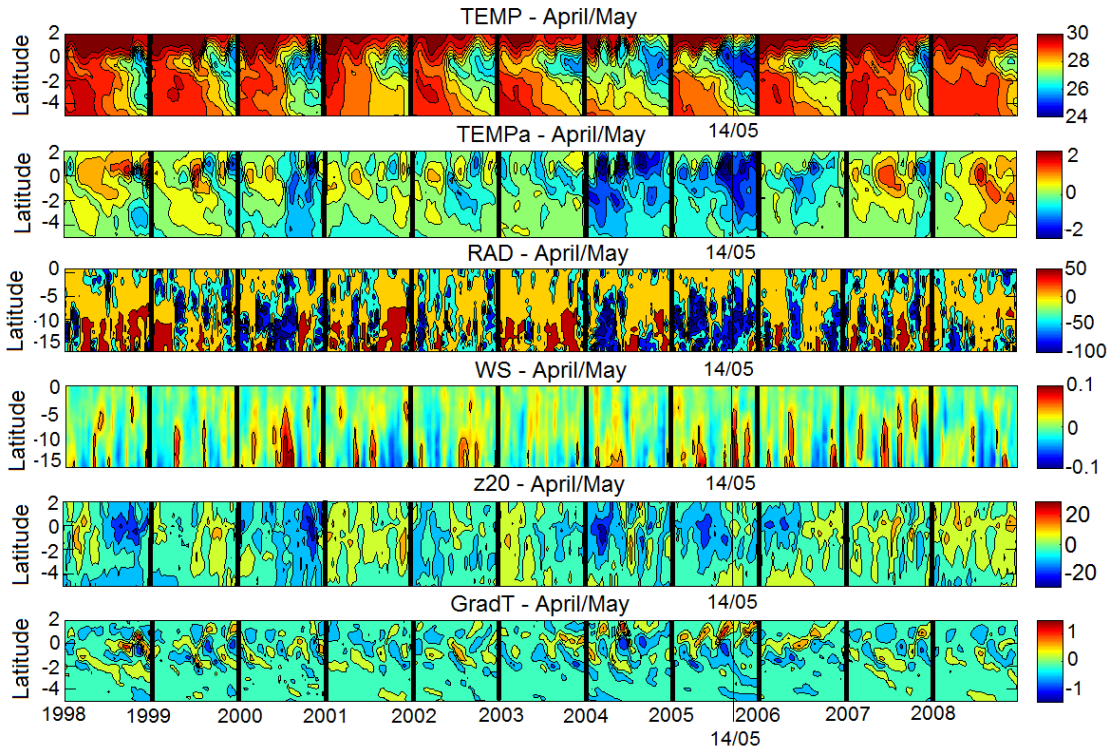
621 April-May are analyzed over the 1998-2008 period (Fig. 12). The intraseasonal wind stress magnitude anomaly
622 during mid-May event appears to be one of the strongest over the whole 1998-2008 period (up to 0.13N.m^{-2}
623 around 15°S and 0.05N.m^{-2} in equatorial region). These strong wind conditions are usually met later in late
624 boreal spring or summer, when the St. Helena Anticyclone strengthens and shifts northward toward the warm
625 hemisphere. The wind intensification in mid-May 2005 was associated with particularly weak RADSW from
626 South Atlantic to the northern equatorial region, suggesting cloud albedo effect during the event which tended to
627 cool the mixed layer. We can notice that the April-May 2005 period was characterized by the weakest mean
628 RADSW.

629 In addition, at the time of the event, the surface waters were already cooled by previous wind bursts (e.g. 20
630 April and 8 May). The SST response to the mid-May event occurred 4-6 days later, inducing the weakest
631 equatorial SST values for April-May season over the whole 1998-2008 period (SST drop of $\sim 3^{\circ}\text{C}$ inducing SST
632 $< 24.8^{\circ}\text{C}$). The cooling also caused an enhanced SST front around 1°N , as shown in Fig. 12 (bottom panel),
633 which was found to be the earliest and strongest one over the 1998-2008 period. This meridional SST gradient
634 was responsible for the wind surface intensification north of the equator (Fig. 11a and Fig. 12, fourth panel)
635 through air-sea interaction mechanisms as described by Leduc-Leballeur et al. (2011). Another SST gradient
636 maximum is found at the end of May 1998 but it was not extended as eastward than during the mid-May 2005
637 event (not shown).

638 When the wind burst occurred on 14 May 2005, the 20°C -isotherm depth in the area was anomalously shallow
639 south of the equator and slightly deeper at the equator (Fig. 12, fifth panel). The thermocline shoaling associated
640 with the Kelvin wave appeared in fact a few days earlier providing favorable subsurface conditions which made
641 the SST response to previous wind bursts (20 April and 8 May) more effective. At the time of the mid-May
642 event, the wave already reached more eastern areas, as shown in previous sections.

643
644 Thus, the particularity of the mid-May 2005 event mainly lies in the i) anomalous atmospheric conditions
645 related to strong St. Helena Anticyclone perturbation; ii) cooling initiated by the succession of previous wind
646 bursts; and iii) favorable subsurface local ocean conditions preconditioned by equatorial waves which shoaled
647 the mixed layer. Another wind burst of comparable intensity occurred at the beginning of May 2000 (Fig. 12,
648 fourth panel) while the thermocline was shallow, causing SST cooling at the equator (Fig. 12, first and second
649 panels). However, the wind strengthening was less sudden than during the mid-May 2005 event and the
650 resulting cooling took place over a less broad region (not shown). In addition, the surface pressure drop in the
651 ITCZ region was not as pronounced as during mid-May 2005 event.

652



653

654 **Figure 12:** Time-latitude diagrams for April-May along the 1998-2008 period, of 2-days average, from top to
 655 bottom i) SST (°C); ii) intraseasonal anomaly of SST (°C); , iii) intraseasonal anomaly of wind stress
 656 magnitude ($N.m^{-2}$) from CFSR fields; iv) intraseasonal anomaly of short-wave radiation surface flux ($W.m^{-2}$)
 657 from CFSR fields; v) intraseasonal anomaly of 20°C-isotherm depth (m) computed from the forced model SST;
 658 vi) intraseasonal anomaly of meridional SST gradient (every 0.5° of latitude), from the forced model; averaged
 659 over 10° W-6° W. The vertical black thin line indicates the date of 14 May, 2005. For details about the
 660 calculations of the anomalies, see Sect. 2.

661

662 6. Summary and discussion

663 In this study, the impact of intraseasonal winds on SST in the far eastern Tropical Atlantic during boreal spring
 664 2005 and 2006 has been investigated from observations and numerical simulation. We first focus our study in
 665 the Cape-Lopez region (CLR), east of 5°E and between the equator and 7° S, where the seasonal and interannual
 666 SST variability is poorly documented. There, the boreal spring (AMJ) season corresponds to a transitional
 667 period between high SST in boreal winter and **low** ST in boreal summer, under the influence of local winds.
 668 Intensified cool SSTs are observed in the coastal upwelling area located around 6° S in the Congo mouth region,
 669 associated with mean alongshore wind conditions. Boreal spring season is in fact characterized by maximum
 670 winds amplitude, influence of which is made more effective by shallow thermocline depth, itself strongly
 671 influenced by remote forcing. The seasonal cycle in the CLR is modulated by strong year-to-year variations, as

672 observed in boreal spring 2005 when cold SST anomaly are associated with shallower-than-average thermocline
673 depth and positive wind speed anomaly.

674 The intraseasonal wind bursts which occurred in boreal spring 2005 and 2006 generated cooling episodes
675 especially around 3°-4° S except for some strongest events when the cooling reached more northern equatorial
676 region, especially during the mid-May and end-May 2005 events. The intensity of the cold events resulted from
677 basin preconditioning by remotely forced shoaling of the thermocline (via Kelvin wave), local mixing (induced
678 by current vertical shear) and upwelling processes in response to strong southerly local winds. For one particular
679 event, on 26-28 May 2005, the net heat flux also tended to cool the surface water, due to enhanced cloud cover
680 which decreased the incoming solar radiations. In the CLR, stronger wind intensification and favorably
681 preconditioned oceanic subsurface conditions in 2005 made the coupling between surface and subsurface ocean
682 processes more efficient than in 2006, resulting in stronger cooling. It should be noted that the occurrence of
683 intraseasonal wind intensification in the CLR is not specific to the boreal spring/summer 2005 and 2006 and is
684 observed every year over the 1998-2008 period of study (not shown). However, their impact on SST variability
685 in the region is modulated depending of the strength of wind intensification and of the subsurface
686 preconditioning. For example, the year 1998, known as a "warm year", is characterized by anomalous warm
687 SST in boreal spring/summer in the CLR., associated with anomalous weak winds and anomalous deep
688 thermocline.

689 The preconditioning of subsurface conditions in the area via Kelvin wave at the dates of the wind bursts
690 depended on the atmospheric conditions in the western part of the basin a few weeks earlier. Previous studies
691 (e.g. Picaut, 1983; Philander, 1990) suggest that the source of an equatorial Kelvin wave is mainly related to a
692 sudden change of the zonal wind in the west. Analysis of atmospheric and oceanic conditions at intraseasonal to
693 daily scale in winter 2005 and 2006 showed that for both years, an Kelvin upwelling wave was initiated in the
694 west while easterly winds were strengthened from either side of the equator just after the ITCZ to be at its
695 southernmost location. This latter was observed one month earlier in 2006 (late February – early March) than in
696 2005 (late March-early April), and was associated with a negative wind stress curl anomaly. In winter 2005, the
697 ITCZ was found south of the equator after a very sudden southward shift and was followed by strong easterlies
698 during ~20 days, while in winter 2006, the ITCZ was found closer to the equator less sharply and during a
699 longer period, followed by weaker easterlies when compared to 2005. These results obtained for the years 2005
700 and 2006 years do not imply that same atmospheric conditions would be observed for winter upwelling Kelvin
701 wave of other years. Especially, the year 2005 was very particular and also exhibited anomalously cold SSTs in
702 the south Atlantic and anomalously warm SSTs in the north Atlantic initiated in fall 2004, signature of a
703 meridional mode (Virmani and Weisberg, 2006; Foltz and Mc. Phaden, 2006; Hormann and Brandt, 2009).

704 Upon impingement at the eastern boundary, the incoming equatorial Kelvin wave excites westward-propagating
705 Rossby waves and poleward propagating coastal Kelvin waves. In 2005, the Kelvin wave reached the coast
706 around mid-May while southerly winds strengthened, allowing the reflected wave to be reinforced by the local
707 wind. This resulted in westward propagation of negative z_{20} and SSH anomalies which, combined with

708 enhanced westward surface currents, provided favorable conditions to westward extension of cold upwelled
709 water from the eastern coast to near 20°W through advection and vertical mixing.

710

711

712 In the second part of the study, we specially focused on the mid-May 2005 event (13 May to 16 May) that was
713 characterized by strong southerly wind strengthening in the eastern Tropical Atlantic Ocean. It was found to be
714 responsible for the sudden and intense SST cooling in the Gulf of Guinea and the CLR, and involved in the early
715 onset of the ACT development in 2005 and therefore **in the early onset** of the WAM. The analysis of
716 atmospheric and oceanic conditions in the Gulf of Guinea associated with this event allowed to show that the
717 mid-May event, controlled by the St. Helena Anticyclone, can be identified as a “decisive event” which
718 triggered the abrupt transition between two wind patterns in the northern Gulf of Guinea. Unusual strong
719 southerly winds induced anomalously strong equatorial cooling which in turns slowed down the overlying wind
720 feedback mechanism and generated stronger than normal southerlies north of the equator through the SST front
721 around 1°N. This triggered the deep atmospheric convection in the Gulf of Guinea at a self-sustaining level and
722 the beginning of coastal precipitation. The time of occurrence of this phenomenon, 15 days earlier than the
723 averaged date (31 May from Leduc-Leballeur et al., 2013), suggests that the mid-May 2005 event was
724 **associated with** anomalous strong moisture flux. The description of atmospheric conditions over the 1998-2008
725 period has shown that the 2005 event was characterized by the strongest surface pressure gradient between the
726 St. Helena high pressures and the low pressures under the ITCZ, inducing strong Hadley cell activity. No similar
727 atmospheric pattern was observed during the whole 1998-2008 period. Another wind burst of comparable wind
728 intensity occurred at the beginning of May 2000. This event also induced a cooling at the equator but the surface
729 pressure decrease in ITCZ region was not as pronounced than during mid-May 2005 event and the SST gradient
730 around 1° N was weaker. In addition to coastal precipitation in the Gulf of Guinea and due to the early cooling
731 in the ACT region, unusually rainfall conditions also occurred between the northeast coast of Brazil and 15° W
732 within the SITCZ, which generally forms in early boreal summer.

733 Finally, this study highlights the impact of a strong southerly wind burst in the eastern tropical Atlantic during
734 boreal spring season, which is a transitional period during which an anomalous strong energy input may tip the
735 energy balance from an equilibrium state toward another one and thus impact the WAM system. The analysis of
736 atmospheric and oceanic conditions during the mid-May 2005 wind event allows to highlight the different
737 processes through which the wind power provided by the wind burst is brought to the ocean: i) direct effect of
738 the wind on the SST in the eastern tropical Atlantic; ii) changes in the trade winds in the western equatorial
739 Atlantic exciting eastward-propagating equatorial Kelvin waves; iii) energy transport via atmospheric gravity
740 waves from South Atlantic; and iv) energy supply to Rossby wave. In addition to unusual atmospheric
741 conditions in mid-May 2005, the ocean response intensity to this event was also enhanced by the subsurface
742 conditions, made favorable by previous wind bursts, either local (e.g. in 6-8 May) or occurring a few weeks
743 before in the West.

744 It is crucial to better describe the atmospheric and oceanic processes at play during such extreme event, notably
745 in order to reduce the well known warm bias in the southeastern tropics in coupled models in both atmospheric
746 and oceanic components (Zeng et al., 1996; Davey et al., 2002; Deser et al., 2006; Chang et al., 2007; Richter
747 and Xie, 2008) as well as in forced ocean-only simulations (e.g. Large and Danabasoglu, 2006). This warm bias
748 is well evidenced in our numerical simulation (Fig. 1&2) and our results clearly show that the cooling episodes
749 were underestimated in the CLR, implying the need to investigate more in depth the oceanic and atmospheric
750 processes at play in this particular region. As the intraseasonal wind bursts are related to the fluctuations of St.
751 Helena Anticyclone, their impact on SST variability in the eastern tropical Atlantic and regional climate
752 suggests the need of better understand the St. Helena Anticyclone variability.

753 It is also important to note that the mid-May 2005 event occurred during an unusually active year. The year
754 2005 exhibited a pronounced meridional mode pattern with strong SST gradient between the two hemispheres.
755 Several authors (Foltz et al., 2006 ; Virmani and Weisberg, 2006 ; Marengo et al., 2008a, 2008b ; Zeng et al.,
756 2008) studied this particular year, marked by anomalously warm SST in the tropical North Atlantic during
757 March-July, the warmest from at least 150 years. This anomalous warming was associated with the most active
758 and destructive hurricane season on record (Foltz et al., 2006; Virmani and Weisberg, 2006) and an extreme and
759 rare drought in the Amazon Basin (Marengo et al., 2008a, 2008b; Zeng et al. 2008; Erfanian et al., 2017). From
760 these authors, primary causes of the anomalous warming in 2005 were a weakening of the northeasterly trade
761 winds and associated decrease in wind-induced latent heat loss as well as changes in shortwave radiation and
762 horizontal oceanic heat advection. This 2005 temperature record is made even more remarkable given that,
763 unlike the 1998's one, it occurred in the absence of any strong El Niño anomaly (Shein, 2006). Some studies
764 (Goldenberg et al., 2001) attribute these SST increases to the Atlantic Multidecadal Oscillation (AMO), while
765 others suggest that climate change may instead be playing the dominant role (Emanuel, 2005; Webster et al.,
766 2005; Mann and Emanuel, 2006; Trenberth and Shea, 2006). Comparable anomalously warm tropical Atlantic
767 SSTs have been observed in 2010 also associated with extreme drought in the Amazon. However, from time
768 series of monthly anomalies constructed for the two basins (North and South Atlantic) by using OISST monthly
769 mean data, Erfanian et al. (2017) show that the warmer-than-usual SSTs in the North Atlantic in 2010 was not
770 associated with colder-than-usual SST in South Atlantic contrarily to 2005 (their Fig. S4e).

771 While the warming in North Tropical Atlantic during 2005 has been investigated by several authors, the cooling
772 in South Atlantic has received less attention. This study highlights the need to further document and monitor the
773 South Atlantic region and the St. Helena Anticyclone, through additional high resolution analysis and
774 observations.

775

776 Acknowledgments:

777 The research leading to these results received funding from the EU FP7/2007-2013 under grant agreement no.
778 603521, PREFACE and from the EU Horizon 2020 under grand agreement no. 2014-633211, AtlantOS. These

779 projects are gratefully acknowledged. We do thank Gildas Cambon for his help and participation on the
780 implementation of ROMS simulations, and Frédéric Marin for his helpful comments.

781

782 **References:**

783

784 Adamec, D., O'Brien, J. J.: The seasonal upwelling in the Gulf of Guinea due to remote forcing, *J. Phys.*
785 *Oceanogr.*, 8, 1050-1060, 1978.

786

787 Battisti, DS.: Dynamics and thermodynamics of a warming event in a coupled tropical atmosphere ocean model,
788 *J. Atmos. Sci.* 45:2889 – 2919, 1988.

789

790 Busalacchi, A., Picaut, J.: Seasonal variability from a model of the tropical Atlantic Ocean, *J. Phys Oceanogr.*,
791 13, 1564-1588, 1983.

792

793 Bourlès, B., Brandt, P., Caniaux, G., Dengler, M., Gouriou, Y., Key, E., Lumpkin, R., Marin, F., Molinari, R.L.,
794 Schmid, C. : African Monsoon Multidisciplinary Analysis (AMMA): Special measurements in the
795 Tropical Atlantic, CLIVAR Exchange Letters, 41 (12 2), International CLIVAR Project Office,
796 National Oceanography Centre, Southampton, United Kingdom, 7–9, 2007.

797

798 Brandt, P., Funk, A., Hormann, V., Dengler, M., Greatbatch, R.J., Toole, J.M.: Interannual atmospheric
799 variability forced by the deep equatorial Atlantic Ocean, *Nature*, 473, 497–500,
800 doi:10.1038/nature10013, 2011.

801

802 Caniaux, G., Giordani, H., Redelsperger, J.-L., Guichard, F., Key, E., Wade, M.: Coupling between the Atlantic
803 cold tongue and the West African monsoon in boreal spring and summer, *J. Geophys. Res.*, 116,
804 C04003, doi:10.1029/2010JC006570, 2011.

805

806 Carton, J. A., Chepurin, G., Cao, X., Giese, B.S.: A simple ocean data assimilation analysis of the global upper
807 ocean 1950 –1995, part 1: Methodology, *J. Phys. Oceanogr.*, 30, 294–309, doi:10.1175/ 1520-
808 0485(2000)030<0294:ASODAA>2.0.CO;2, 2000a.

809

810 Carton, J. A., Chepurin, G., Cao, X.: A simple ocean data assimilation analysis of the global upper ocean 1950–
811 1995, part 2: Results, *J. Phys. Oceanogr.*, 30,311–326, doi:10.1175/1520-0485(2000)
812 030<0311:ASODAA>2.0.CO;2, 2000b.

813

814 Carton, J. A., and Giese, B.S.: A reanalysis of ocean climate using simple ocean data assimilation (SODA),
815 *Mon. Weather Rev.*, 136 ,2999–3017, doi:10.1175/2007MWR1978.1, 2008.

816

817 Colin, C.: Sur la variabilité dans le Golfe de Guinée: Nouvelles considérations sur les mécanismes d'upwelling,
818 Ph.D. thesis, Mus. Natl. d'Hist. Nat., Paris, 1989.
819

820 Chang, C.-Y., Carton, J.A., Grodsky, S.A., Nigam, S.: Seasonal climate of the tropical Atlantic sector in the
821 NCAR Community Climate System Model 3: Error structure and probable causes of errors, *J. Climate*,
822 20, 1053–1070, 2007.
823

824 Chelton, D. B., deSzoeke, R.A., Schlax, M. G. , Naggar, K. E., Siwertz, N.: Geographical variability of the first-
825 baroclinic Rossby radius of deformation, *J. Phys. Oceanogr.*, 28, 433–460, 1998.
826

827 Dai, A., and Trenberth, K.E.: Estimates of freshwater discharge from continents: Latitudinal and seasonal
828 variations, *J. Hydrometeorol.*, 3, 660–687, 2002.
829

830 Danabasoglu, G., Large, W.G., Tribbia, J.J., Gent, P.R., Briegleb, B.P.: Diurnal Coupling in the Tropical
831 Oceans of CCSM3, *Journal of Climate*, 19, 2347-2365, 2006.
832

833 Davey, M., Huddleston, M., Sperber, K.R., et al.: STOIC: A study of coupled model climatology and variability
834 in tropical ocean regions, *Clim. Dynam.*, 18, 403-420, 2002.
835

836 Debreu, L., Marchesiello, P., Penven, P., Cambon, G.: Two-way nesting in split-explicit ocean models:
837 algorithms, implementation and validation, *Ocean Modelling*, 49-50, 1-21, 2012.
838

839 De Coëtlogon, G., Janicot, S., Lazar, A.: Intraseasonal variability of the ocean-atmosphere coupling in the Gulf
840 of Guinea during boreal spring and summer, *Q. J. R. Meteorol. Soc.*, 136, 426–441, doi:10.1002/qj.554,
841 2010.
842

843 Denamiel, C., Budgell, W.P., Toumi, R.: The Congo River plume: Impact of the forcing on the far-field and
844 near-field dynamics, *J. Geophys. Res. Oceans*, 118, 964–989, doi:10.1002/jgrc.20062, 2013.
845

846 Deser, C., Capotondi, A., Saravanan, R., Phillips, A.: Tropical Pacific and Atlantic climate variability in
847 CCSM3, *J. Climate*, 19, 2451–2481, 2006.
848

849 Djakouré, S., Penven, P., Bourlès, B., Veitch, J., Koné, V.: Coastally trapped eddies in the north of the Gulf of
850 Guinea, *J. Geophys. Res. Oceans*, 119, 6805–6819, doi:10.1002/2014JC010243, 2014.
851

852 Emanuel, K.: Increasing destructiveness of tropical cyclones over the past 30 years, *Nature*, 436, 686-688, 2005.
853

854 Erfanian, A., Wang, G., Fomenko, L.: Unprecedented drought over tropical South America in 2016:
855 significantly under-predicted by tropical SST, *Scientific reports*, 7:5811, doi: 10.1038/s41598-
856 017_05373-2, 2017.

857

858 Foltz, G. R., Grodsky, S. A., Carton, J. A., McPhaden, M. J.: Seasonal mixed layer heat budget of the tropical
859 Atlantic Ocean, *J. Geophys. Res.*, 108, 3146, doi:10.1029/2002JC001584, 2003.

860

861 Foltz, G.R. and McPhaden, M.J.: Unusually warm sea surface temperatures in the tropical North Atlantic during
862 2005, *Geophys. Res. Lett.*, 33: doi: 10.1029/2006GL027394. issn: 0094-8276, 2006.

863

864 Fritts, D. C.: Wave saturation in the middle atmosphere: A review of theory and observations, *Rev. Geophys.*,
865 22, 275–308, 1984.

866

867 Gentemann, C.L., Wentz, F.J., Brewer, M., et al.: Passive Microwave Remote Sensing of the Ocean: an
868 Overview, *Oceanography from Space, Revisited*, edited by V. Barale, J. Gower, and L. Alberotanza,
869 13–33. Heidelberg: Springer, 2010.

870

871 Giese, B.J, Harrison, D.E.: Aspects of the Kelvin wave response to episodic wind forcing, *J. Geophys. Res.*, 95:
872 7289 – 7312, 1990.

873

874 Giordani, H., Caniaux, G., Voldoire, A.: Intraseasonal mixed-layer heat budget in the equatorial Atlantic during
875 the cold tongue development in 2006, *J. Geophys. Res.: Oceans*, 118(2):650-671. doi:
876 10.1029/2012JC008280, 2013.

877

878 Goldenberg, S.B., Landsea, C.W., Mestas-Nuñez, A.M., Gray, W.M.: The Recent Increase in Atlantic Hurricane
879 Activity: Causes and Implications, *Sciences*, Vol. 293, Issue 5529, pp. 474-479, doi:
880 10.1126/science.1060040, 2001.

881

882 Grodsky, S. A., Carton, J. A.: The Intertropical Convergence Zone in the South Atlantic and the Equatorial Cold
883 Tongue, *J. Climate*, 16, 723–733, 2003.

884

885 Haidvogel, D.B., Beckmann, A.: *Numerical Ocean Circulation Modeling*, Imperial College Press, London; 320
886 pp., 1999.

887

888 Herbert, G., Bourlès, B., Penven, P., Grelet, J.: New insights on the upper layer circulation north of the Gulf of
889 Guinea, *J. Geophys. Res.: Oceans*, 121, doi:10.1002/2016JC011959, 2016.

890

891 Hormann, V., Brandt, P.: Upper equatorial Atlantic variability during 2002 and 2005 associated with equatorial
892 Kelvin waves, *J. Geophys. Res.*, 114: C03007, doi:10.1029/2008JC005101, 2009.
893

894 Illig, S., Dewitte, B., Ayoub, N., du Penhoat, Y., Reverdin, G., Mey, P.D., Bonjean, F., Lagerloef, G.S.E.:
895 Interannual long equatorial waves in the tropical Atlantic from a high-resolution ocean general
896 circulation model experiment in 1981-2000, *J. Geophys. Res.: Oceans*, 109:C02022. doi: 10.1029/
897 2003JC001771, 2004.
898

899 Jouanno, J., Marin, F., duPenhoat, Y., Sheinbaum, J., Molines, J.M.: Seasonal heat balance in the upper 100m of
900 the Equatorial Atlantic Ocean, *J. Geophys. Res.: Oceans*, 116:C09003. doi: 10.1029/2010JC006912,
901 2011.
902

903 Jouanno, J., Marin, F., duPenhoat, Y., Molines, J.M.: Intraseasonal Modulation of the Surface Cooling in the
904 Gulf of Guinea, *J. Phys. Oceanogr.*, 43(2):382-401. doi: 10.1175/JPO-D-12-053.1, 2013.
905

906 Krishnamurti, T. N., Pasch, R.J., Ardanuy, P.: Prediction of African waves and specification of squall lines,
907 *Tellus*, 32, 215-231, 1980.
908

909 Leduc-Leballeur, M., Eymard, L., de Coëtlogon, G.: Observation of the marine atmospheric boundary layer in
910 the Gulf of Guinea during the 2006 boreal spring, *Q. J. R. Meteorol. Soc.*, 137: 992 – 1003, 2011.

911 Leduc-Leballeur, M., de Coëtlogon, G., Eymard, L.: Air – sea interaction in the Gulf of Guinea at intraseasonal
912 time-scales: Wind bursts and coastal precipitation in boreal spring, *Q. J. R. Meteorol. Soc.*, 139, 387–
913 400, doi:10.1002/qj.1981, 2013.
914

915 Lübbecke, J.F., Burls, N.J., Reason, C.J.C., McPhaden, M.J.: Variability in the South Atlantic Anticyclone and
916 the Atlantic Nino Mode, *J. Climate*, 27, doi: 10.1175/JCLI-D-14-00202.1, 2014.
917

918 Mann, M. E., and Emanuel, K.A.: Atlantic hurricane trends linked to climate change, *Eos, Trans. Amer.*
919 *Geophys. Union*, 87, 233–244, 2006.
920

921 Marengo, J. A., Nobre, C.A., Tomasella, J., Oyama, M.D., De Oliveira, G.S., De Oliveira, R., Camargo, H.,
922 Alves, L.M., Brown, I.F. : The drought of Amazonia in 2005, *J. Climate*, 21, 495-516, 2008a.
923

924 Marengo, J.A., Nobre, C.A., Tomasella, J., Cardoso, M.F., Oyama, M.D.: Hydro-climatic and ecological
925 behaviour of the drought of amazonia in 2005, *Philosophical transactions of the Royal society of*
926 *London, Biological sciences*, v.21, p.1-6, 2008b.
927

928 Marin, F., Caniaux, G., Boulès, B., Giordani, H., Gouriou, Y., Key, E.: Why were sea surface temperatures so
929 different in the Eastern Equatorial Atlantic in June 2005 and 2006, *J. Phys. Oceanogr.*, 39, 1416–1431,
930 doi:10.1175/2008JPO4030.1, 2009.

931

932 Materia, S., Gualdi, S., Navarra, A., Terray, L.: The effect of Congo River freshwater discharge on Eastern
933 Equatorial Atlantic climate variability, *Clim. Dynam.*, 39(9-10), 2109–2125, doi:10.1007/s00382-012-
934 1514-x, 2012.

935

936 McCreary, J.: Eastern tropical ocean response to changing wind systems with application to El Nino, *J. Phys.*
937 *Oceanogr.*, 6, 632-645, 1976.

938

939 McCreary, J., Picaut, J., Moore, D.: Effects of the remote annual forcing in the eastern tropical Atlantic Ocean,
940 *J. Mar. Res.*, 42, 45–81, 1984.

941

942 Merle, J. : Conditions hydrologiques saisonnières de la marge continentale du Gabon et du Congo (de 10°N a
943 60°S) Etude descriptive, *Dot. Sci. O.R.S.T.O.M. Pointe-Noire*, 27 : 1-20, 1972.

944

945 Merle, J., Fieux, M., Hisard, P.: Annual signal and interannual anomalies of sea surface temperature in the
946 eastern equatorial Atlantic Ocean, *Deep Sea Res.*, 26,77–101, 1980.

947

948 Mitchell, T. P., Wallace, J.M.: The annual cycle in equatorial convection and sea surface temperature, *J.*
949 *Climate*, 5, 1140–1156, 1992.

950

951 Moore, D.W.: Planetary-gravity waves in an equatorial ocean, PhD Thesis, Harvard University, 201 pp., 1968.

952

953 Moore, D.W., and Philander, S.G.H.: Modeling of the tropical ocean circulation, *The Sea*, Vol. 6, Wiley
954 Interscience, New York, N.Y., pp. 316-361, 1977.

955

956 Moore, D. W., Hisard, P., McCreary, J. P., Merle, J., O'Brien, J. J., Picaut, J., Verstraete, J. M., Wunsch, C.:
957 Equatorial adjustment in the eastern Atlantic, *Geophys. Res. Lett.*, 5, 637-640, 1978.

958

959 Nguyen, H., Thorncroft, C. D., Zhang, C.: Guinean coastal rainfall of the West African Monsoon, *Q.J.R.*
960 *Meteorol. Soc.*, 137: 1828–1840. doi:10.1002/qj.867, 2011.

961 Nicholson, S.E., Dezfuli, A.K.: The relationship of rainfall variability in western equatorial Africa to the tropical
962 oceans and atmospheric circulation. Part I: The boreal spring, *J. Climate*, 26(1), 45–65, 2013.

963 Nobre, P., Shukla, J.: Variations of sea surface temperature, wind stress, and rainfall over the tropical Atlantic
964 and South America, *J. Climate*, 9 : 2464 – 2479, 1996.

965

966 Okumura, Y., and Xie, S.P.: Interaction of the Atlantic equatorial cold tongue and the African monsoon, *J.*

967 *Climate*, 17, 3589–3602, 2004.

968

969 Okumura, Y., Xie, S.P.: Some overlooked features of tropical Atlantic climate leading to a new Niño-like

970 phenomenon, *J. Climate*, 19(22), 5859–5874, doi:10.1175/JCLI3928.1, 2006.

971

972 Ostrowski, M., Da Silva, J. C. B., Bazik-Sangolay, B.: The response of sound scatterers to El-Niño and La Niña-

973 like oceanographic regimes in the southeastern Atlantic, *ICES J. Mar. Sci.*, 66 (6), 1063-1072, doi:

974 [10.1093/icesjms/fsp102](https://doi.org/10.1093/icesjms/fsp102), 2009.

975

976 Penven, P., Marchesiello, P., Debreu, L., Lefevre, J.: Software tools for pre- and post-processing of oceanic

977 regional simulations, *Environ. Modell. Software*, 23, 2008 660–662, 2008.

978

979 Peter, A.-C., Le Hénaff, M., du Penhoat, Y., Menkès, C., Marin, F., Vialard, J., Caniaux, G., Lazar, A.: A model

980 study of the seasonal mixed layer heat budget in the equatorial Atlantic, *J. Geophys. Res.*, 111, C06014,

981 doi: 10.1029/2005JC003157, 2006.

982

983 Philander, S., and Pacanowski, R.: A model of the seasonal cycle in the Tropical Atlantic Ocean, *J. Geophys.*

984 *Res.*, 91, 14, 192–14, 206, 1986.

985

986 Philander, S.G.: *El Nino, La Nina and the Southern Oscillation*, Academic Press, 293 pp., 1990.

987

988 Picaut, J.: Propagation of the seasonal upwelling in the eastern equatorial Atlantic, *J. Phys. Oceanogr.*, 13, 18–

989 37, doi: 10.1175/1520-0485, 1983.

990

991 Picaut, J.: On the dynamics of the thermal variations in the Gulf of Guinea, *Oceanogr. Trop.*, 19 (2) : 127-53,

992 1984.

993

994 Piton, B. : Les courants sur le plateau continental devant Pointe-Noire (Congo), *Documents scientifiques*,

995 ORSTOM, Brest, n°47, 37 p., 1988.

996

996 Polo, I., Lazar, A., Rodriguez-Fonseca, B., Arnault, S.: Oceanic Kelvin waves and tropical Atlantic

997 intraseasonal variability: 1. Kelvin wave characterization, *J. Geophys. Res.*, 113, C07009, doi: 10.1029/

998 2007JC004495, 2008.

999

1000 Redelsperger, J. L., et al. : AMMA: Une étude multidisciplinaire de la mousson Ouest-Africaine, *Meteorologie*,

1001 54,22–32, doi:10.4267/2042/20098, 2006.

1002

1003 Richter, I. and Xie, S.-P.: On the origin of equatorial Atlantic biases in coupled general circulation models,
 1004 *Clim. Dynam.*, 1:587–598, doi : 10.1007/s00382-008-0364-z, 2008.

1005 Rouault, M., Servain, J., Reason, C. J. R. , Bourlès, B., Rouault, M. J. , Fauchereau, N.: Extension of PIRATA
 1006 in the tropical south-east Atlantic: An initial one-year experiment, *Afr. J. Mar. Sci.*,31(1),63–71,
 1007 doi:10.2989/AJMS.2009.31.1.5.776, 2009.

1008

1009 Saha, S., Moorthi, S., Pan, H.-L., Wu, W., Wang, J., Nadiga, S., Tripp, P., Kistler, R., Woollen, J., Behringer,
 1010 D., Liu, H., Stokes, D., Grumbine, R., Gayno, G., Wang, J., Hou, Y.T., Chuang, H.-Y., Juang, H.-M.
 1011 H., Sela, J., Iredell, M., Treadon, R., Kleist, D., Van Delst, P., Keyser, D., Derber, J., Ek, M., Meng, J.,
 1012 Wei, H., Yang, R., Lord, S., Van Den Dool, H., Kumar, A., Wang, W., Long, C., Chelliah, M., Xue, Y.,
 1013 Huang, B., Schemm, J.-K., Ebisuzaki, W., Lin, R., Xie, P., Chen, M., Zhou, S., Higgins, W., Zou, C.-Z.
 1014 Z., Liu, Q., Chen, Y., Han, Y., Cucurull, L., Reynolds, R.W., Rutledge, G., Goldberg, M. : The NCEP
 1015 climate forecast system reanalysis, *Amer. Meteor. Soc.*, 91, 1015-1057, 2010.

1016

1017 Schouten, M. W., Matano, R. P., Strub, T. P.: A description of the seasonal cycle of the equatorial Atlantic from
 1018 altimeter data, *Deep Sea Res., Part I*, 52, 477–493, doi:10.1016/j.dsr.2004.10.007, 2005.

1019

1020 Servain, J., Picaut, J., Merle, J.: Evidence of remote forcing in the equatorial Atlantic Ocean, *J. Phys. Oceanogr.*,
 1021 12, 457–463, 1982.

1022

1023 Shein, K. A.: State of the climate in 2005, *Bull. Am. Meteorol. Soc.*, 87, s1–s102, doi: 10.1175/BAMS-87-6-
 1024 shein, 2006.

1025

1026 Shchepetkin, A., McWilliams, J.C.: The Regional Oceanic Modeling System (ROMS): A split-explicit, free-
 1027 surface, topography-following-coordinate ocean model, *Ocean Modell.* 9, 347–404, 2005.

1028

1029 Thorncroft, C. D., Nguyen, H., Zhang, C., Peyrillé, P.: Annual cycle of the West African monsoon: regional
 1030 circulations and associated water vapour transport, *Q. J. R. Meteorol. Soc.*, 137, 129-147,
 1031 doi:10.1002/qj.728, 2011.

1032

1033 Trenberth, K.E., Shea, D.J.: Atlantic hurricanes and natural variability in 2005, *Geophys. Res. Lett.*, vol. 33,
 1034 L12704, doi: 10.1029/2006GL026894, 2006.

1035

1036 Virmani, J. I., and Weisberg, R.H.: The 2005 hurricane season: An echo of the past or a harbinger of the future?,
 1037 *Geophys. Res. Lett.*, 33, L05707, doi: 10.1029/2005GL025517, 2006.

1038

1039 Wade, M., Caniaux, G., du Penhoat, Y.: Variability of the mixed layer heat budget in the eastern equatorial
1040 Atlantic during 2005–2007 as inferred using Argo floats, *J. Geophys. Res.*, 116, C08006, doi:
1041 10.1029/2010JC006683, 2011.

1042

1043 Yu, L., Jin, X., Weller, R.A.: Role of net surface heat flux in seasonal variations of sea surface temperature in
1044 the tropical Atlantic ocean, *J. Climate*, 19, 6153–6169, 2006.

1045

1046 Waliser, D. E., and Gautier, C.: A satellite-derived climatology of the ITCZ, *J. Climate*, 6, 2162–2174, 1993.

1047

1048 Wauthy, B. : Introduction à la climatologie du Golfe de Guinée, *Oceanogr. Trop.*, 18, 103–138, 1983.

1049

1050 Webster, P.J., Holland, G. J., Curry, A., Chang, H.R.: Changes in tropical cyclone number, duration, and
1051 intensity, in warming environment, *Science*, 309, 1844-1846, 2005.

1052

1053 Wentz, F.J., and Meissner, T.: Algorithm Theoretical Basis Document (ATBD), version 2, AMSR-E Ocean
1054 Algorithm, Remote Sensing Systems Tech. Rep., RSS 121599A-1, 55 pp., 2000.

1055

1056 White, R.H. and Toumi, R.: River Flow and Ocean Temperatures: The Congo River, *J. Geophys. Res. -Oceans*,
1057 119, 25016–2517, doi:10.1002/2014JC009836, 2014.

1058

1059 Zebiak, S.: Air-sea interaction in the equatorial Atlantic region, *J. Climate*, 6(8), 1567–1586, doi:10.1175/1520-
1060 0442(1993)006<1567:AIITEA>2.0.CO;2, 1993.

1061

1062 Zeng, N., Dickinson, R.E., Zeng, X.: Climatic impact of Amazon deforestation-A mechanistic model study, *J.*
1063 *Climate*, 9, 859–883, 1996.

1064

1065 Zeng, N., Dickinson, R.E., Zeng, X.: Causes and impacts of the 2005 Amazon drought, *Env. Res. Lett.*, 3, doi:
1066 10.1088/1748-9326/3/1/014002, 2008.